

ConceptSeg-R1: Segment Any Concept via Meta-Reinforcement Learning

Yuan Zhao^{1,2*}, Youwei Pang^{3*}, Jiaming Zuo², Wei Ji⁴,
Kailai Zhou³, Bin Fan⁵, Yunkang Cao⁶, Lihe Zhang^{1‡},
Xiaofeng Liu⁴, Huchuan Lu¹, Weisi Lin³, Dacheng Tao³, Xiaoqi Zhao^{3‡}

¹Dalian University of Technology, China

²X3000 Inspection Co., Ltd

³Nanyang Technological University, Singapore

⁴Yale University, USA

⁵Northwestern Polytechnical University, China

⁶Hunan University, China

*equal contribution. ‡corresponding authors.

Recent progress in promptable segmentation has shifted visual perception from object-level localization toward concept-level understanding. However, the notion of a concept remains under-specified, making it unclear whether current methods truly generalize beyond category recognition. In this work, we formalize generalized concept segmentation through a three-level taxonomy consisting of context-independent (CI), context-dependent (CD), and context-reasoning (CR) concepts, which reveals a clear capability gap across increasing levels of cognitive complexity. To address this challenge, we propose ConceptSeg-R1, a unified framework that reformulates concept segmentation as rule-induced concept grounding. At the core of our method is Meta-GRPO, a meta-reinforcement learning mechanism that learns transferable task rules from visual demonstrations and verifies them through proxy reasoning. The inferred reasoning states are then translated into segmentation-ready concept prompts via a lightweight concept translation module, enabling deductive application to target images. A shortcut routing strategy further preserves the native efficiency of segmentation models on simple cases. To systematically evaluate generalized concept segmentation, we conduct extensive experiments across diverse CI, CD, and CR concept segmentation benchmarks spanning natural, industrial, medical and reasoning-intensive domains. Without bells and whistles, ConceptSeg-R1 achieves strong performance across the full concept hierarchy while maintaining the native capability of promptable segmentation backbones. As an initial step toward segmenting any concept, we hope ConceptSeg-R1 can serve as a practical baseline for advancing segmentation from object-level prediction toward concept-level understanding.

Project Page: <https://ntu-ai4x.github.io/ConceptSeg-R1>

Source Code: <https://github.com/NTU-AI4X/ConceptSeg-R1>

1 Introduction

Visual segmentation aims to localize regions that satisfy a user-specified semantic requirement. Over the past decade, the field has evolved from closed-set pixel classification with task-specific supervision [1–4] toward open-world, prompt-driven perception. The Segment Anything Model (SAM) [5] marked a major milestone by unifying segmentation through geometric prompts such as points and boxes, enabling strong zero-shot transfer across diverse domains. More recently, SAM 3 [6] extended this paradigm to promptable concept segmentation, where targets can be specified using open-vocabulary concept prompts rather than fixed labels. This progress

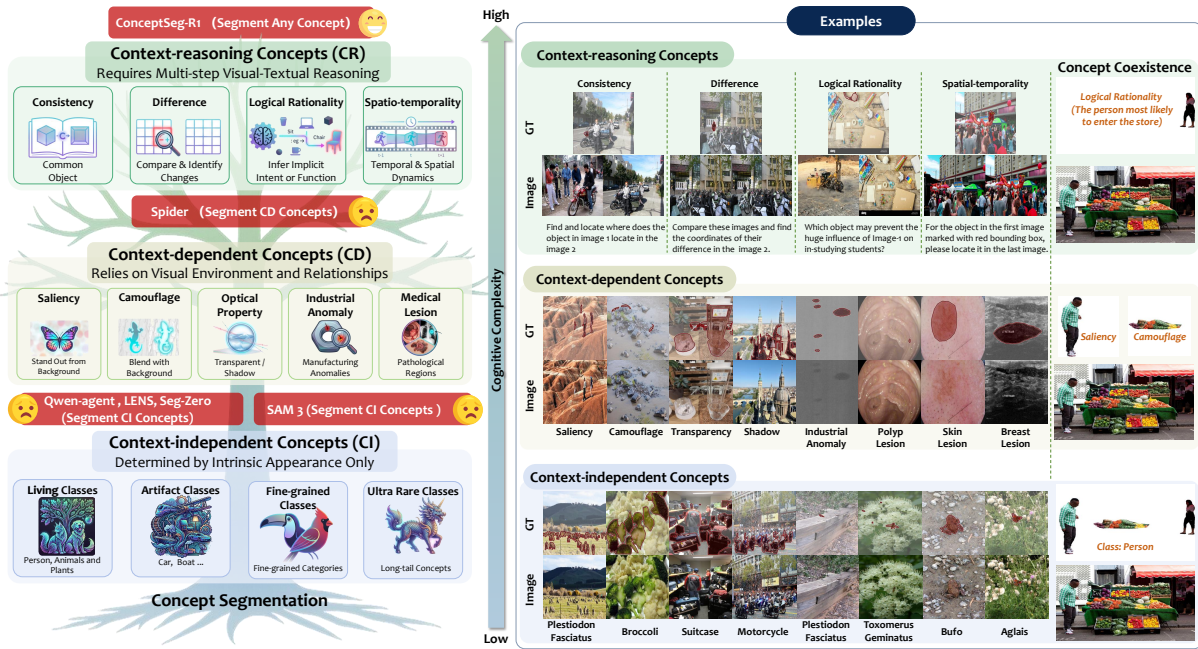


Figure 1. Concept segmentation tree with representative CI, CD, and CR concepts arranged by cognitive complexity. Existing promptable segmentation models mainly handle CI concepts, while context-oriented and reasoning-enhanced methods partially cover CD or CR concepts. ConceptSeg-R1 targets the full concept hierarchy toward segmenting any concept. See § A for details.

suggests a promising path toward more general segmentation systems. However, a central question remains unresolved: *what exactly is a concept in concept segmentation?* Existing works often equate concepts with text-addressable object categories, yet many real-world targets are defined not only by category identity, but also by contextual relations or reasoning requirements. Without a principled concept taxonomy, it remains difficult to determine whether a model truly generalizes beyond category recognition toward broader concept-level understanding.

Concept categorization has long been studied in philosophy and cognitive science, where concepts are commonly distinguished as context-independent or context-dependent [7–9]. Similar distinctions have recently emerged in visual understanding and segmentation research [10, 11]. However, these studies are developed for task-specific models or narrowly defined prompting settings. In this work, we revisit concept segmentation from the perspective of general-purpose segmentation foundation models and methods based on multi-modal large language models (MLLMs), where concept understanding must account for varying levels of contextual dependency and cognitive complexity.

As illustrated in Fig. 1, we organize generalized concept segmentation into a three-level concept hierarchy. The first level is **Context-Independent Concepts (CI)**, whose identities are determined primarily by intrinsic appearance and semantic attributes. General living, artifact, fine-grained and long-tail ultra rare classes belong to this regime, where targets can often be recognized without strong contextual contrast cues. Promptable and generalist segmentation models [5, 6, 12] are naturally strong in this setting. The second level is **Context-Dependent Concepts (CD)**, where targets are defined through their relation to the environment, such as saliency, camouflage, transparency, shadows, industrial anomalies, or medical lesions. These concepts require perception of contextual contrast or domain-specific structure rather than object identity alone. This perspective is closely related to Spider [10], although it mainly studies context-dependent concepts under visual prompting rather than a unified text-and-vision interactive framework. The third level is **Context-Reasoning Concepts (CR)**, which require explicit reasoning over visual and textual evidence, often involving cross-image correspondence,

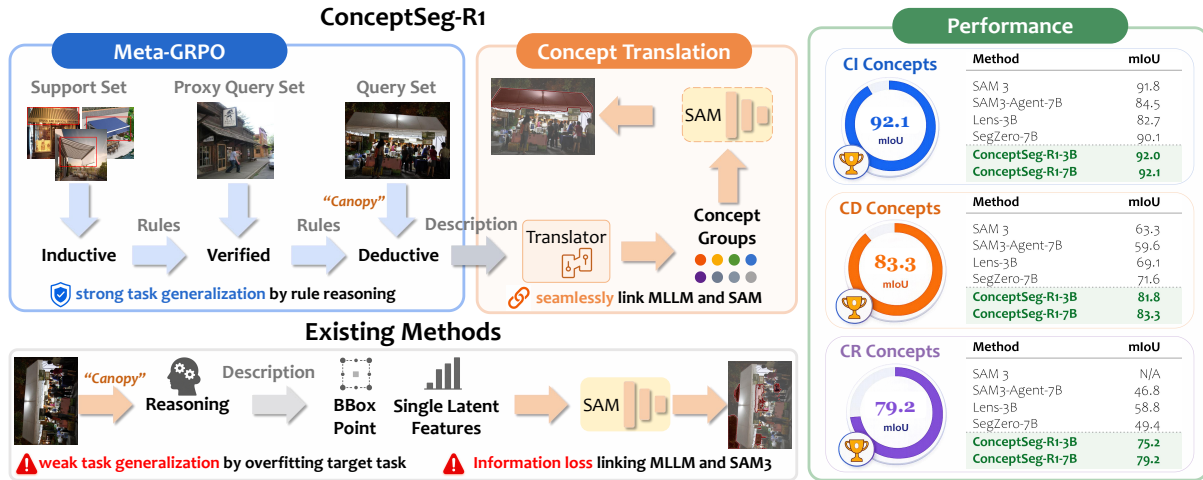


Figure 2. Workflow and performance comparison. ConceptSeg-R1 employs Meta-GRPO to induce rules and deductive reasoning, which are converted into lossless prompts for SAM via concept translation, enabling robust full-spectrum concept segmentation.

temporal cues, or functional semantics. These CR concepts go beyond contextual perception and require reasoning over relationships or functional dependencies across observations. Recent MLLM-based frameworks [13–16] begin to explore this regime by integrating visual reasoning into segmentation. Nevertheless, a unified concept hierarchy connecting CI, CD, and CR for general-purpose segmentation foundation models remains missing.

Despite recent progress, existing methods still face two fundamental limitations, as illustrated by the “existing methods” pathway in Fig. 2. First, many approaches follow a reasoning → description → interface → segmentation pipeline, where rich semantics are compressed into low-bandwidth representations such as bounding boxes or short descriptions, causing a semantic bottleneck between reasoning and segmentation. Second, most methods perform inference case by case rather than inducing transferable task rules from demonstrations. Instruction-tuning [13, 17, 18], agent-based [6, 19, 20], and reinforcement learning-based approaches [15, 16, 21] improve reasoning consistency but still optimize instance-level trajectories instead of task-level induction. Consequently, they remain brittle under cross-task transfer, out-of-distribution shifts, and reasoning-intensive scenarios requiring concept inference from visual demonstrations.

In this work, we address these limitations with **ConceptSeg-R1**, a unified framework that reformulates generalized concept segmentation as a closed-loop process of task induction → rule verification → concept translation → promptable segmentation, as illustrated in Fig. 2. Instead of solving each example independently, ConceptSeg-R1 leverages reference images to induce transferable task rules and apply them to the query image. The first key component is **Meta-GRPO**, a meta-learning variant of group relative policy optimization that introduces a split-reference strategy with support examples and proxy queries. This mechanism enables the model to induce reusable rules from visual demonstrations, verify them on proxy queries, and apply them deductively to target images. The second key component is the **Concept Translation Module (CTM)**, which maps MLLM hidden states into implicit concept groups that can be injected into the segmentation prompt space, preserving rich reasoning signals for pixel-level execution. Finally, a **Shortcut Router** routes simple CI-style cases directly to SAM 3 while activating the full reasoning pipeline only when deeper contextual or logical inference is required. In this way, ConceptSeg-R1 unifies efficient promptable segmentation with context-aware concept grounding and rule-induced reasoning.

As shown in Fig. 2, we evaluate ConceptSeg-R1 on a total of 16 benchmarks spanning CI, CD, and CR concepts. By spanning the cognitive spectrum from fundamental recognition to

visuospatial dependency modeling and high-level visual-textual reasoning, this hierarchical evaluation validates the model’s effectiveness in bridging the gap between basic perception and complex task induction across diverse natural, industrial, and medical scenarios. In addition, ConceptSeg-R1 achieves competitive results on widely used benchmarks such as Cityscapes [22] and ReasonSeg [17], further validating its generalization and reasoning capability. Taken together, these results suggest that generalized concept segmentation should be studied not merely as static category recognition, but as a unified problem of context-aware concept grounding, rule induction, and executable visual reasoning.

2 Related Work

Promptable Segmentation. Recent advances have expanded visual segmentation from task-specific mask prediction to open-world interactive perception. SAM [5] established a strong foundation by unifying diverse segmentation tasks through geometric prompts, such as points and boxes. Building on this paradigm, SAM 3 [6] introduced promptable concept segmentation, enabling segmentation with noun-phrase concepts and open-vocabulary semantic prompts. Recent methods further extend this capability to complex instructions: SAM3-I [13] improves instruction following for SAM 3, while agent-based or reasoning-enhanced frameworks, such as AgentRVOS [23] and CoT-Seg [24], incorporate MLLMs and Chain-of-Thought reasoning for temporally or semantically complex queries. Despite these advances, most existing systems still follow a sequential reasoning-to-prompt pipeline, where rich intermediate reasoning is compressed into boxes, points, short descriptions, or single latent representations. This semantic bottleneck limits their ability to execute fine-grained reasoning at the mask level, especially for context-dependent and reasoning-intensive concepts.

MLLMs with Reinforcement Learning. Multi-modal large language models (MLLMs) have recently been introduced into segmentation to enhance reasoning and instruction-following ability. Early reasoning segmentation frameworks, such as LISA [17] and GLaMM [25], mainly rely on supervised fine-tuning to connect MLLM hidden states with mask decoders. Although effective for language-mask alignment, supervised training alone often struggles with out-of-distribution concepts, ambiguous instructions, and complex visual-textual reasoning. To improve reasoning consistency and spatial grounding, recent works have explored reinforcement learning for segmentation. Seg-Zero [15] introduces GRPO-based optimization for reasoning-chain guided segmentation, while LENS [16] studies unified reinforced reasoning for segmentation. Subsequent methods, such as Seg-R1 [21], further incorporate dense spatial or mask-level feedback to improve grounding quality. These works demonstrate the potential of reinforcement learning for reasoning segmentation, but they primarily optimize instance-level reasoning trajectories, where each query is solved independently, leaving task-level transfer and rule induction insufficiently explored.

Meta-Learning and Rule Induction. Learning to adapt from limited examples has long been studied as a core objective of meta-learning. Classical methods such as MAML [26] and Reptile [27] optimize model initialization for fast adaptation, while recent LLM studies connect this ability with in-context learning, where models infer task patterns from demonstrations without parameter updates. Works such as MetaICL [28] and MAML-en-LLM [29] improve few-shot generalization in language models. However, existing studies mainly focus on text-centric tasks or passive demonstration following, whereas generalized concept segmentation requires models to infer reusable visual rules from support examples, verify them under proxy contexts, and apply them to unseen target images. This paper brings this perspective into MLLM-based segmentation by formulating concept segmentation as rule-induced concept grounding, where visual demonstrations, proxy verification, and reinforced optimization jointly improve generalization across CI, CD, and CR concepts.

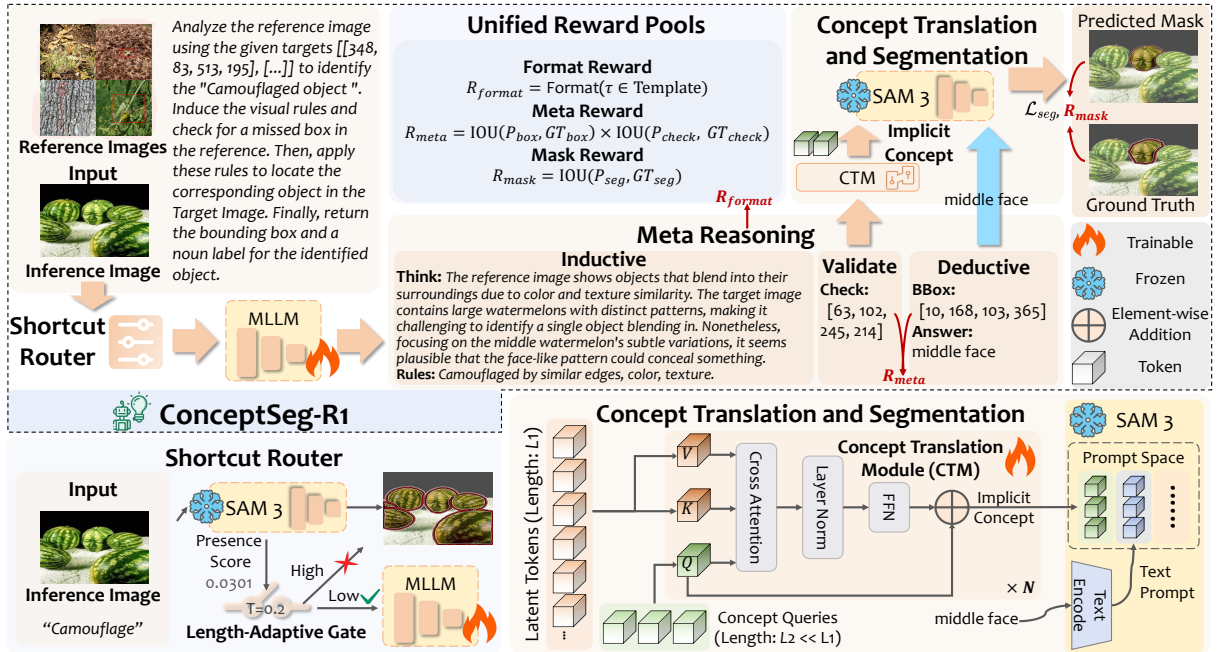


Figure 3. Overview of the ConceptSeg-R1 architecture. (§ 3.1)

3 ConceptSeg-R1

3.1 Overall architecture

We propose ConceptSeg-R1, a unified framework for generalized concept segmentation. The architecture follows a four-step paradigm: **task induction** \rightarrow **rule verification** \rightarrow **concept translation** \rightarrow **promptable segmentation**. As illustrated in Fig. 3, ConceptSeg-R1 utilizes an MLLM as the reasoning engine and SAM 3 as the segmentation backbone. The framework takes as input a mosaic of reference images (partitioned into a Support Set and a Proxy Query Set), a target inference image as the actual query, and a textual prompt. A Shortcut Router adaptively determines whether full reasoning is needed: for high-confidence cases, SAM 3 is directly invoked via a fast path, bypassing meta-reasoning. Otherwise, the model induces task-level rules from the Support Set, verifies them on the Proxy Query Set, and applies them to the target image. Finally, the Concept Translation Module (CTM) maps these linguistic deductions into multi-dimensional implicit concept groups, serving as high-fidelity prompts for SAM 3 to generate precise pixel masks.

3.2 Meta-GRPO

We introduce Meta-GRPO, a meta-learning variant of GRPO [30], to improve in-context learning and out-of-distribution (OOD) generalization for generalized concept segmentation. Unlike conventional segmentation methods that solve each image independently, Meta-GRPO internalizes meta-learning within a single visual context window through a Split-Reference Strategy. Given visual demonstrations, the model is encouraged to induce transferable task rules, verify them under proxy contexts, and deductively apply them to the target query image I . This formulation connects reinforcement learning with in-context meta-learning, enabling the model to move beyond instance-level reasoning toward rule-based concept grounding.

Split-Reference Strategy. To leverage multi-image context while maintaining computational efficiency, we organize the visual inputs into a mosaic-based reference structure. Given a target image I , which serves as the actual query, and a textual prompt \mathcal{T} , we construct a reference set $\mathcal{R} = \{S, Q\}$ as a $K \times K$ mosaic image to reduce memory overhead. Within the mosaic, S denotes

the Inductive Support Set, from which the model infers task-level rules, while Q denotes the Proxy Query Set, which is used for intermediate rule verification. The MLLM first performs induction over S , then localizes the corresponding target in Q to validate the induced rules, and finally applies the verified rules to I by predicting object box coordinates and a descriptive linguistic answer.

Meta Reward. To encourage rule-based reasoning rather than shortcut memorization or reward hacking [31], we design a meta reward that jointly evaluates proxy-level verification and target localization quality. The model samples trajectories τ from the concatenated visual-textual context:

$$\tau \sim \pi_{\theta}(\cdot \mid [S, Q, I, \mathcal{T}]) \quad (1)$$

The meta reward is defined as

$$R_{meta} = \text{IoU}(P_{box}, GT_{box}) \times \text{IoU}(P_{check}, GT_{check}) \quad (2)$$

where P_{box} and GT_{box} denote the predicted and ground-truth boxes for I , and P_{check} and GT_{check} denote the boxes for Q . By coupling proxy deduction with target segmentation, Meta-GRPO rewards trajectories that rely on transferable, context-aware task rules rather than direct memorization of individual samples.

3.3 Concept Translation

To eliminate the information bottleneck between high-level reasoning and segmentation execution, we develop a lightweight Concept Translation Module (CTM) with near-linear complexity. CTM converts the rich Chain-of-Thought (CoT) hidden states from the MLLM into multi-dimensional implicit concept groups that can be injected into the latent prompt space of SAM 3, enabling richer reasoning-to-mask transfer.

Specifically, given the MLLM output tokens $\mathbf{H} \in \mathbb{R}^{L_1 \times C}$, where L_1 is the token length, we initialize a compact set of learnable concept queries $\mathbf{C} \in \mathbb{R}^{L_2 \times C}$ with a much smaller length $L_2 \ll L_1$. The concept queries attend to the reasoning tokens through cross-attention:

$$\mathbf{Z} = \text{CrossAttn}(\mathbf{C}, \mathbf{H}, \mathbf{H}) \quad (3)$$

where $\mathbf{Z} \in \mathbb{R}^{L_2 \times C}$ denotes the extracted implicit concept groups. These groups summarize multi-faceted semantic attributes from the reasoning trajectory, such as appearance, spatial relations, relative scale, and functional properties. Meanwhile, the final short linguistic description is encoded by the SAM 3 text encoder to obtain explicit prompt embeddings \mathbf{E}_{text} . The implicit concept groups are then prepended to the explicit embeddings in the SAM 3 latent prompt space:

$$\mathbf{P} = [\mathbf{Z}; \mathbf{E}_{text}] \quad (4)$$

where \mathbf{P} serves as the final prompt representation for mask prediction. Since CTM uses a small number of concept queries rather than the full MLLM token sequence, its cross-attention cost is $O(L_1 L_2 C)$ and becomes near-linear in L_1 when L_2 is fixed and much smaller than L_1 .

Compared with conventional sequential pipelines that suffer from semantic disconnect, CTM translates complex reasoning states into segmentation-compatible visual guidance through a unified trainable interface. This replaces discrete tool-calling with continuous concept prompts, better preserving reasoning information while balancing segmentation accuracy and inference efficiency.

3.4 Training and Inference

We adopt a progressive training and adaptive inference strategy to balance reasoning capacity and computational efficiency. Training consists of two stages: CTM warm-up with supervised segmentation loss, followed by Meta-GRPO optimization with unified rewards. During inference, a lightweight Shortcut Router built upon the native confidence mechanism of SAM 3 decides whether to accept the direct SAM 3 prediction or activate the full ConceptSeg-R1 reasoning pipeline.

Training Stage I: Supervised Fine-Tuning. In the first stage, both the MLLM and SAM 3 are frozen, and only the CTM parameters are optimized. This stage aligns MLLM reasoning features with the latent prompt space of SAM 3, allowing implicit concept groups to serve as effective segmentation prompts. The optimization objective is the standard segmentation loss:

$$\mathcal{L}_{seg} = \mathcal{L}_{dice}(P_{seg}, GT_{seg}) + \mathcal{L}_{focal}(P_{seg}, GT_{seg}) \quad (5)$$

where P_{seg} and GT_{seg} denote the predicted and ground-truth masks, respectively.

Training Stage II: Cognitive Reinforcement Learning. In the second stage, the reasoning policy π_θ is optimized with Meta-GRPO under a structured CoT template consisting of <rule>, <check>, <think>, <bbox>, and <answer> tags. The unified reward pool combines format correctness, mask quality, and meta-level rule verification:

$$R_{uni} = R_{format} + R_{mask} + R_{meta} \quad (6)$$

The format and mask rewards are defined as:

$$R_{format} = \mathbf{1}[t_\tau \models \mathcal{T}_{CoT}] \quad R_{mask} = \text{IoU}(P_{seg}, GT_{seg}) \quad (7)$$

where t_τ denotes the generated reasoning response of trajectory τ , and $t_\tau \models \mathcal{T}_{CoT}$ indicates that the response satisfies the required CoT template. Here, R_{meta} is the proxy-target reward defined in § 3.2, which couples proxy rule verification with target localization quality. The final training objective combines Meta-GRPO optimization with the segmentation loss:

$$\mathcal{L}_{train} = \mathcal{L}_{GRPO}(R_{uni}, D_{KL}) + \mathcal{L}_{seg} \quad (8)$$

where KL divergence term D_{KL} acts as a standard regularization constraint, preventing the current policy from deviating excessively from the reference policy. This ensures linguistic stability and prevents catastrophic forgetting by anchoring the reasoning trajectories within a plausible distribution.

Adaptive Inference with Shortcut Router. At inference time, the Shortcut Router first uses the native SAM 3 prediction branch to obtain a presence score s , which reflects the confidence that the queried concept can be directly localized without additional reasoning. The decision threshold T is adjusted according to instruction complexity:

$$T = \text{CLIP}(0.1 \times 2^{\ell(\mathcal{T})-1}, \min = 0, \max = 1) \quad (9)$$

where $\ell(\mathcal{T})$ denotes the normalized word count of the instruction \mathcal{T} , and $\text{CLIP}(\cdot)$ denotes the clamping function used to constrain the output within a predefined range. A smaller T is produced for short atomic instructions, making SAM 3 predictions easier to accept through the shortcut path when $s \geq T$. In contrast, longer queries yield a larger T , imposing a stricter acceptance criterion and activating the full ConceptSeg-R1 pipeline when native SAM 3 confidence is insufficient. This adaptive mechanism allows simple CI-style queries to be handled efficiently while reserving full reasoning capacity for complex CD and CR concepts.

Table 1. Quantitative comparison on diverse CI, CD, and CR concept segmentation benchmarks. Detailed results for diverse classes in CI concepts and more evaluation metrics are provided in § E.

Method	CI Concepts				CD Concepts								CR Concepts								Mean		
	Diverse Classes		Optical Property		Camouflage		Saliency		Industrial Anomaly		Medical Lesion		Consistency		Difference		Logical Rationality		Spatio-temporality				
	$F_\beta^w \uparrow$	mIoU \uparrow	$F_\beta^w \uparrow$	mIoU \uparrow	$F_\beta^w \uparrow$	mIoU \uparrow	$F_\beta^w \uparrow$	mIoU \uparrow	$F_\beta^w \uparrow$	mIoU \uparrow	$F_\beta^w \uparrow$	mIoU \uparrow	$F_\beta^w \uparrow$	mIoU \uparrow	$F_\beta^w \uparrow$	mIoU \uparrow	$F_\beta^w \uparrow$	mIoU \uparrow	$F_\beta^w \uparrow$	mIoU \uparrow	$F_\beta^w \uparrow$	mIoU \uparrow	
SAM 3 [6]	89.5	91.8	85.6	86.4	51.3	61.4	38.1	59.0	51.5	66.2	36.3	48.9	-	-	-	-	-	-	-	-	-	-	-
<i>MLLM + SAM</i>																							
SAM3-Agent-3B [6]	55.1	72.3	47.5	62.0	45.4	64.8	59.5	72.1	20.6	49.1	17.1	41.4	20.3	43.2	3.1	30.9	20.3	46.9	10.2	40.5	29.9	52.3	
SAM3-Agent-7B [6]	76.8	84.5	68.3	74.3	58.9	71.7	74.4	80.2	31.5	49.0	25.1	42.5	26.7	46.8	26.7	53.1	29.3	53.3	13.5	37.1	43.1	59.3	
LENS-3B [16]	74.4	82.7	56.0	65.4	58.1	73.1	76.9	81.1	51.3	60.2	56.0	69.1	26.7	55.2	25.6	56.8	19.5	55.1	43.7	68.2	48.8	66.7	
Seg-Zero-7B [15]	86.8	90.1	67.1	73.1	75.0	81.1	72.8	78.6	51.4	57.1	60.2	69.8	16.1	49.6	5.5	49.2	9.8	49.3	7.2	49.3	45.2	64.7	
ConceptSeg-R1-3B	89.9	92.0	85.7	86.5	83.7	87.7	89.0	90.5	61.5	71.0	69.0	77.4	63.9	77.0	52.7	71.8	46.6	68.5	64.7	79.1	70.7	80.1	
ConceptSeg-R1-7B	89.9	92.1	85.7	86.5	84.8	88.3	92.7	93.5	66.7	74.1	72.3	79.3	70.1	81.0	57.0	75.0	60.2	76.7	69.8	81.8	74.9	82.8	

4 Experiments

4.1 Settings

Datasets. We evaluate ConceptSeg-R1 on a diverse set of concept segmentation benchmarks spanning context-independent (CI), context-dependent (CD), and context-reasoning (CR) concepts. These benchmarks cover natural, industrial, medical, and reasoning-intensive scenarios, enabling a comprehensive assessment of out-of-distribution generalization across different levels of cognitive complexity. In addition, we include representative generic segmentation and reasoning-oriented benchmarks, such as Cityscapes [22] and ReasonSeg [17], to verify whether ConceptSeg-R1 preserves the generic segmentation capability of SAM 3 and generalizes to external reasoning-grounded settings. Complete dataset descriptions and evaluation protocols are provided in § B.

Implementation Details and Metrics. We employ the Qwen2.5-VL series [32] as the reasoning backbone and SAM 3 as the segmentation head, using both 3B and 7B variants in our experiments. Training is conducted on 8 NVIDIA H800 GPUs utilizing the DeepSpeed engine to optimize memory and training efficiency. Following previous works [6, 10, 15, 16], we report four widely adopted segmentation metrics: weighted F-measure (F_β^w), mean Intersection-over-Union (mIoU), generalized IoU (gIoU) and cumulative IoU (cIoU). All results are reported in percentage (%). More details and metrics are provided in § C and § E.

4.2 Comparison

Performance on CI, CD and CR Concepts. As summarized in Tab. 1, ConceptSeg-R1 achieves consistently strong performance across the full CI-CD-CR spectrum. On CI concepts, SAM 3 first shows strong segmentation capability, even outperforming several MLLM-based models such as LENS and SegZero. However, directly pairing SAM 3 with an MLLM without careful design can lead to noticeable performance degradation, as evidenced by the lower results of SAM3-Agent-3B and SAM3-Agent-7B. In contrast, ConceptSeg-R1 preserves the strong segmentation capability of SAM 3 while achieving the best overall performance on diverse CI concepts. On CD concepts, ConceptSeg-R1 shows clear advantages across diverse domains, including optical properties, camouflage, industrial anomaly, and medical lesions. Notably, ConceptSeg-R1-3B achieves 77.4 mIoU on the medical lesion benchmark, outperforming the larger Seg-Zero-7B model. On CR concepts, SAM 3 is not designed to handle scenarios that require reasoning across multiple observations, and therefore cannot directly perform such tasks. Among MLLM-based methods, ConceptSeg-R1 shows the most significant performance advantage on CR concepts, consistently achieving the best results on consistency, difference, logical rationality, and spatio-temporality reasoning concepts.

Performance on Cityscapes and ReasonSeg. As shown in Tab. 2, ConceptSeg-R1 maintains strong zero-shot segmentation performance on the Cityscapes benchmark, improving the overall mIoU from 60.6 to 62.6 without task-specific training. In addition, Tab. 3 shows that

Table 2. Comparison of ConceptSeg-R1 and SAM 3 on Cityscapes under the zero-shot setting, evaluated using the mIoU metric. Since official semantic segmentation scripts for SAM 3 are unavailable, results are reported under the same inference settings as ConceptSeg-R1 for fair comparison.

Method	Road	Side.	Build.	Wall	Fence	Pole	T.Light	T.Sign	Veget.	Terra.	Sky	Person	Rider	Car	Truck	Bus	Train	Motor.	Bicycle	Mean
SAM 3 [6]	91.4	82.2	84.4	19.1	45.4	61.1	64.7	67.2	88.4	5.7	92.6	76.2	39.3	87.6	42.6	54.3	29.2	46.6	72.9	60.6
ConceptSeg-R1-3B	97.9	82.6	83.9	18.8	47.3	60.8	60.2	66.6	87.3	7.2	93.7	74.8	39.4	89.4	52.8	62.3	42.6	50.5	72.1	62.6
Δ Gains	+6.5	+0.4	-0.5	-0.3	+1.9	-0.3	-4.5	-0.6	-1.1	+1.5	+1.1	-1.4	+0.1	+1.8	+10.2	+8.0	+13.4	+3.9	-0.8	+2.0

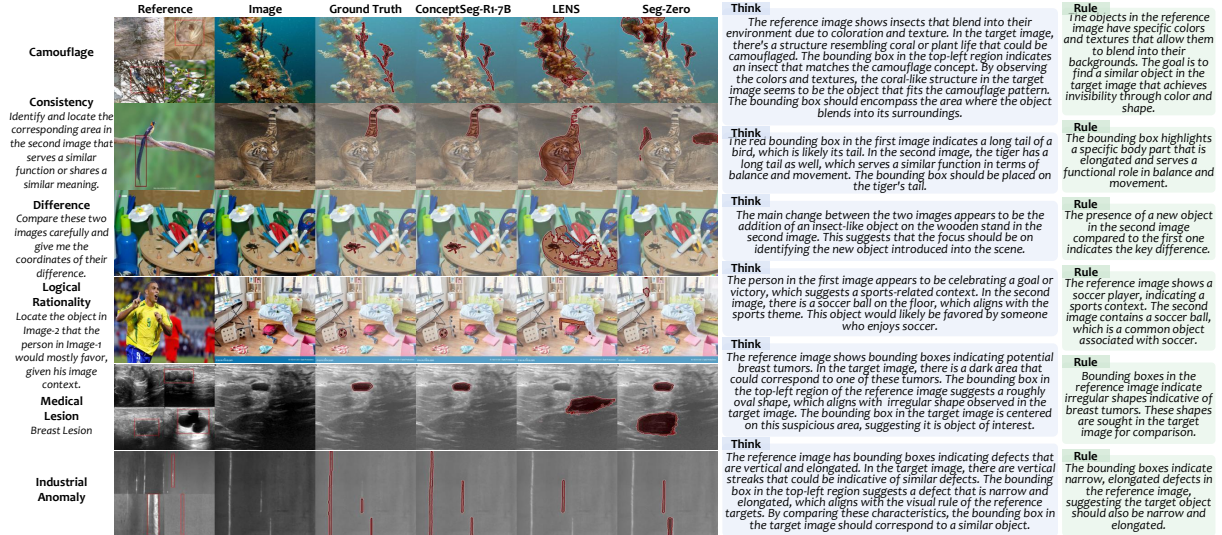


Figure 4. Qualitative comparison across different concepts. See § K for more visualization results.

ConceptSeg-R1 achieves state-of-the-art performance on the ReasonSeg benchmark. Notably, our method achieves both the highest gIoU and cIoU on ReasonSeg-Test without task-specific fine-tuning, demonstrating strong reasoning capability and robust generalization to external reasoning-oriented segmentation settings.

Qualitative Comparison. As shown in Fig. 4, ConceptSeg-R1 shows superior visual grounding compared to LENS and Seg-Zero, highlighting three key advantages: *I) Rule-based Generalization:* For camouflaged object and medical lesion concepts (see the 1st and 5th rows in Fig. 4), ConceptSeg-R1 produces more precise boundaries while competing models often generate fragmented masks, indicating that Meta-GRPO effectively induces transferable task rules for domain-specific perception. *II) Cross-image Reasoning:* In consistency and difference reasoning tasks, ConceptSeg-R1 correctly identifies functional correspondences and inter-class differences across images, suggesting that the split-reference strategy enables stable cross-image reasoning. *III) High-Fidelity Execution:* In logical reasoning scenarios, the concept translation module preserves rich reasoning states for segmentation, avoiding the semantic loss commonly observed in methods relying on coarse prompts. This lossless concept translation also empowers our model to excel in multi-object segmentation and demonstrates a superior capacity to rectify suboptimal ground-truth labels, such as missing targets or imprecise boundaries in industrial anomaly scenarios (see the 6th row in Fig. 4). To further demonstrate the prompt understanding capability of ConceptSeg-R1, Fig. 5 presents representative predictions under concept coexistence scenarios. We observe that ConceptSeg-R1 learns to switch segmentation targets accurately according to different prompts, without relying on a specific query image. In particular, for CR concepts, the model infers that dehydration

Table 3. Zero-shot performance on ReasonSeg [17]. “†” denotes models fine-tuned on the ReasonSeg training set.

Method	Publication	ReasonSeg-Val		ReasonSeg-Test	
		gIoU ↑	cIoU ↑	gIoU ↑	cIoU ↑
LISA-7B† [17]	CVPR’24	52.9	54.0	55.6	56.9
InstructSeg-3B† [18]	ICCV’25	61.9	65.2	–	–
LENS-3B† [16]	AAAI’26	62.1	64.9	57.2	58.0
SAM4MLLM-7B [33]	ECCV’24	46.7	48.1	–	–
Seg-Zero-3B [15]	arXiv’25	58.2	53.1	56.1	48.6
Seg-Zero-7B [15]	arXiv’25	62.6	62.0	57.5	52.0
SAM-R1-7B [34]	NeurIPS’25	64.0	55.8	60.2	54.3
SAM3-Agent-7B [6]	ICLR’26	62.2	49.1	63.0	53.5
DPAD-7B [35]	CVPR’26	63.1	61.2	57.7	54.4
ConceptSeg-R1-3B	–	62.8	54.0	61.2	49.3
ConceptSeg-R1-7B	–	64.4	55.1	63.0	59.3

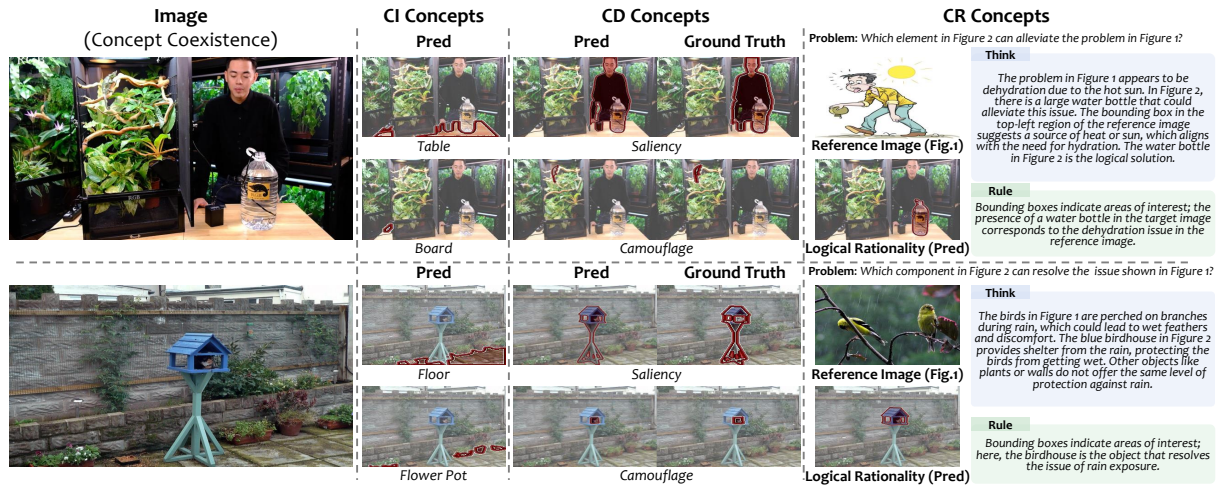


Figure 5. Visualization of concept coexistence results generated by ConceptSeg-R1. The same query image is segmented differently under varying reference instructions.

Table 4. Ablation studies of ConceptSeg-R1-3B across the full CI-CD-CR concept spectrum.

Method	CI Concepts		CD Concepts						CR Concepts						Mean							
	Diverse Classes		Optical Property		Camouflage		Saliency		Industrial Anomaly		Medical Lesion		Consistency				Difference		Logical Rationality		Spatio-temporality	
	$F_p^w \uparrow$	mIoU \uparrow	$F_p^w \uparrow$	mIoU \uparrow	$F_p^w \uparrow$	mIoU \uparrow	$F_p^w \uparrow$	mIoU \uparrow	$F_p^w \uparrow$	mIoU \uparrow	$F_p^w \uparrow$	mIoU \uparrow	$F_p^w \uparrow$	mIoU \uparrow	$F_p^w \uparrow$	mIoU \uparrow	$F_p^w \uparrow$	mIoU \uparrow	$F_p^w \uparrow$	mIoU \uparrow		
(a) Architecture																						
SAM 3	89.5	91.8	85.6	86.4	51.3	61.4	38.1	59.0	51.5	66.2	36.3	48.9	-	-	-	-	-	-	-	-	-	
+ MLLM (SFT)	89.2	91.4	85.8	86.5	80.6	85.6	87.2	88.4	55.9	61.9	57.3	67.5	28.3	56.8	15.9	53.1	18.3	53.4	21.7	56.8	54.0	70.1
+ GRPO	89.4	91.6	85.8	86.5	76.4	82.3	86.4	87.8	55.5	62.4	54.5	65.0	25.2	54.2	21.4	53.5	32.2	60.0	30.3	61.4	55.7	70.5
+ Concept Translations	89.5	91.8	85.8	86.5	82.0	86.5	90.7	91.8	56.5	63.7	61.8	70.2	58.5	73.4	31.4	54.9	45.6	66.5	57.6	75.5	65.9	75.8
+ Meta-GRPO	89.9	92.0	85.7	86.5	83.7	87.7	89.0	90.5	61.5	71.0	69.0	77.4	63.9	77.0	52.7	71.8	46.6	68.5	64.7	79.1	70.7	80.1
(b) Meta-GRPO Component																						
w/o Meta Reward	89.5	91.8	85.8	86.5	82.4	86.6	89.2	90.4	60.0	66.6	68.1	76.9	59.6	74.1	51.7	71.1	41.8	66.8	65.4	79.5	69.3	79.0
w/o Meta Reasoning	89.9	92.0	85.7	86.5	83.6	87.6	90.3	91.3	60.4	70.4	66.1	76.2	61.3	75.5	48.5	68.8	36.2	63.3	63.5	78.5	68.5	79.0
ConceptSeg-R1	89.9	92.0	85.7	86.5	83.7	87.7	89.0	90.5	61.5	71.0	69.0	77.4	63.9	77.0	52.7	71.8	46.6	68.5	64.7	79.1	70.7	80.1
(c) Training Stage																						
One-stage (Only RL)	89.5	91.7	85.8	86.5	84.9	87.4	90.5	91.7	64.2	70.6	69.0	75.0	56.7	71.7	36.0	61.1	44.2	67.5	53.1	72.7	67.4	77.6
Two-stage (SFT + RL)	89.9	92.0	85.7	86.5	83.7	87.7	89.0	90.5	61.5	71.0	69.0	77.4	63.9	77.0	52.7	71.8	46.6	68.5	64.7	79.1	70.7	80.1

requires water and that birds exposed to rain require shelter, selecting the water bottle and birdhouse accordingly, which demonstrates reasoning-driven target selection guided by reference understanding and problem interpretation.

4.3 Ablation Study

As shown in Tab. 4, we conduct ablation experiments to analyze contributions of key designs in ConceptSeg-R1. See § F, G, H, I for more results.

Architecture Evolution. We first establish a strong baseline by introducing an MLLM with supervised fine-tuning (SFT), where the model generates geometric bounding boxes as intermediate prompts for SAM 3. This simple integration already achieves performance that exceeds competing methods in Tab. 1, ensuring subsequent design choices lead to convincing performance improvements. Building upon this baseline, introducing GRPO yields a modest improvement in mean mIoU (70.1 \rightarrow 70.5), suggesting reinforcement learning improves reasoning stability. Replacing geometric prompts with the Concept Translation Module (CTM) leads to a substantial gain (70.5 \rightarrow 75.8), highlighting the benefit of translating reasoning states into dense concept representations. The full Meta-GRPO configuration further improves performance to 80.1 mean mIoU, demonstrating the proposed design choices contribute consistent and convincing performance improvements across diverse concepts.

Meta-GRPO Component Analysis. We further analyze the mechanisms of Meta-GRPO by removing key components. Replacing the Meta-Reward with a standard bounding box IoU reward leads to clear performance degradation on out-of-distribution datasets, indicating that

without the meta-reward constraint, the model tends to memorize training cases rather than induce transferable task rules. Similarly, bypassing the meta-reasoning process results in a noticeable drop in accuracy, particularly on CR concepts, where rule verification is essential for resolving complex visual-textual ambiguities. Overall, removing either the meta-reward or the meta-reasoning component consistently reduces performance, demonstrating that both reward design and reasoning verification are necessary for stable rule induction and robust generalization.

Training Strategy. We further compare one-stage reinforcement learning with the proposed two-stage training scheme. The two-stage setting achieves higher overall performance and more stable results across CI, CD, and CR concepts, confirming the importance of initializing the model with supervised instruction alignment before reinforcement learning.

5 Conclusion

We present ConceptSeg-R1, a unified framework for generalized concept segmentation across context-independent (CI), context-dependent (CD), and context-reasoning (CR) concepts. By introducing rule-induced concept grounding and reference-conditioned reasoning, ConceptSeg-R1 enables segmentation to adapt to diverse contextual and reasoning requirements beyond static category recognition. Extensive experiments demonstrate strong performance across a wide range of natural, industrial, medical, and reasoning-intensive scenarios, while preserving native capability and efficiency of promptable segmentation backbones. As an initial step toward segmenting any concept, ConceptSeg-R1 provides a practical baseline for advancing segmentation from object-level prediction toward concept-level understanding. We hope this work will encourage future research on unified concept segmentation, particularly in more complex multi-modal and real-world settings.

Appendix

A	Concept Definition	13
A.1	Context-Independent Concepts (CI)	13
A.2	Context-Dependent Concepts (CD)	13
A.3	Context-Reasoning Concepts (CR)	13
A.4	Unified Concept Definition from the CR Perspective	14
A.5	Prompt-Based Instantiation of Concept Rules	14
A.6	Visualizing Dependency and Reasoning Conditions	15
B	Hierarchical Concept Segmentation Benchmark Suite	16
C	Implementation Details	18
C.1	Stage 1: Supervised Fine-Tuning	19
C.2	Stage 2: Cognitive Reinforcement Learning	19
D	Prompt Templates	19
D.1	Standard Instruction Template	19
D.2	Token Representations and Semantic Placeholders	20
D.3	Compositional Sensitivity and Mosaic Processing	20
E	Comprehensive Quantitative Results	20
F	Reward Configuration Evaluation	22
G	Routing Strategy Evaluation	22
H	Concept Query Sensitivity	23
I	Reference Robustness and Configuration	24
J	Beyond Mask Accuracy: Decomposing Reasoning Segmentation	25
K	Qualitative Visualization	25
L	Limitations and Future Works	26

A Concept Definition

We provide formal definitions and boundary conditions for the three levels of concept complexity used throughout the paper: context-independent (CI), context-dependent (CD), and context-reasoning (CR) concepts. These definitions aim to clarify the semantic scope of each concept category by characterizing the source of concept identity: intrinsic attributes for CI concepts, contextual relations for CD concepts, and higher-order reasoning structures for CR concepts.

A.1 Context-Independent Concepts (CI)

A concept is defined as context-independent if its identity can be determined primarily by intrinsic visual appearance and semantic attributes, without requiring explicit reasoning about surrounding context or relationships. Typical examples include common object classes, man-made artifacts, and fine-grained biological species. CI concepts correspond to appearance-driven recognition and represent the baseline level of perception in generalized segmentation. Formally, a segmentation target belongs to the CI category if the mapping between an input image x and its segmentation output y can be determined from a single observation:

$$y = f_{\text{CI}}(x) \quad (10)$$

In this setting, the target concept has a self-contained semantic identity. The prediction does not depend on external reference images, relational constraints, or logical inference beyond appearance-based recognition.

A.2 Context-Dependent Concepts (CD)

A concept is defined as context-dependent if its identification requires understanding relationships between the target and its surrounding environment. These relationships may involve foreground-background contrast, transparency, occlusion, or domain-specific context such as industrial anomalies or medical lesions. In contrast to CI concepts, the identity of the target cannot be determined solely from intrinsic appearance, but instead emerges from its interaction with environmental context. Representative examples of CD concepts include saliency, where the target stands out from the background; camouflage, where the target blends into its surroundings; transparency or shadows, where the target appearance is altered by contextual visual interactions; industrial anomalies, whose definition depends on manufacturing conditions and requirements; and medical lesions, which must be interpreted relative to anatomical context. Formally, the segmentation of a CD concept depends on the contextual structure in which the concept is semantically situated:

$$y = f_{\text{CD}}(x, C_x) \quad (11)$$

where C_x denotes contextual information within the image, such as background structure, spatial relationships, or domain-specific conditions. The role of C_x is not merely auxiliary. It is part of the semantic definition of the concept itself. This formulation emphasizes that the segmentation decision relies on relational perception rather than isolated object recognition.

A.3 Context-Reasoning Concepts (CR)

A concept is defined as context-reasoning if its semantic identity is specified by higher-order reasoning structures, such as cross-instance correspondence, scene differences, temporal relations, or other rules derived from reference information. Unlike CD concepts, whose identities arise from local or domain-specific relations within an environment, CR concepts are defined by abstract relational rules that may span multiple observations, modalities, time steps, or logical constraints. Typical reasoning scenarios include consistency reasoning to establish correspondences across multiple images, difference reasoning to identify changes between

scenes, logical reasoning to determine functional relationships, and spatio-temporal reasoning to track objects across time or viewpoints. These represent the higher level of cognitive complexity in the proposed taxonomy because their identities are not directly tied to fixed appearance or local context, but to inferred relational structures. Formally, the semantic specification of a CR concept can be expressed as a two-step process of rule abstraction and application:

$$\gamma = \Psi(m_1, m_2, \dots, m_k) \quad (12)$$

$$y = f_{\text{CR}}(x, \gamma) \quad (13)$$

where $\{m_1, m_2, \dots, m_k\}$ denotes a set of mixed-type reference inputs (such as support images and guiding texts). $\Psi(\cdot)$ denotes the reasoning operator that abstracts these references into a defining rule γ , and $f_{\text{CR}}(\cdot)$ applies this rule on the target input x . This formulation explicitly captures the rule-defined nature of CR concepts.

A.4 Unified Concept Definition from the CR Perspective

From the perspective of CR concepts, the preceding CI, CD, and CR formulations can be unified by treating γ as the variable component that determines the source of concept identity. Specifically, the general rule-based formulation in equation (13) can be extended to all three concept levels by defining γ as follows:

$$\gamma = \begin{cases} \emptyset & \text{for CI concepts} \\ C_x & \text{for CD concepts} \\ \Psi(m_1, m_2, \dots, m_k) & \text{for CR concepts} \end{cases} \Rightarrow y = \begin{cases} f_{\text{CI}}(x, \emptyset) \\ f_{\text{CD}}(x, C_x) \\ f_{\text{CR}}(x, \Psi(m_1, m_2, \dots, m_k)) \end{cases} \quad (14)$$

Here, \emptyset indicates that no additional defining rule is introduced.

A.5 Prompt-Based Instantiation of Concept Rules

The unified formulation above provides a direct motivation for the prompt-based design of our model. While γ specifies the intrinsic concept source of semantic identity, our model instantiates it dynamically through a prompt-conditioned rule η derived from visual references and textual guidance. As stated in § 3.2, given a target image \mathcal{I} and a textual prompt \mathcal{T} , we construct a visual reference set \mathcal{R} . The concept rule is then obtained by:

$$\eta = \Psi(\mathcal{R}, \mathcal{T}) \quad (15)$$

$$y = f(\mathcal{I}, \eta) \quad (16)$$

where $\Psi(\cdot)$ instantiates the prompt-conditioned rule from the reference inputs, and $f(\cdot, \eta)$ applies this rule to the target image. A critical question arises: *How can a unified framework accommodate such divergent abstraction levels, ranging from isolated appearance filtering to complex logical deduction?* This is achieved by formulating textual instructions and visual references as complementary sources for concept rule induction.

Instead of pre-defining separate relational structures for different concept categories, the same formulation $\eta = \Psi(\mathcal{R}, \mathcal{T})$ allows the induced rule η to vary according to the semantic or reasoning demand specified by \mathcal{T} . Based on the aforementioned concept definitions, this prompt-based formulation therefore manifests as three distinct rule induction demands under a unified framework. Here, \rightsquigarrow denotes the expected implicit abstraction behavior induced by the unified operator $\Psi(\cdot)$, rather than an explicitly pre-constructed input structure. The symbol \leftrightarrow is used to indicate the intended semantic interaction or relational dependency between different sources, rather than a specific architectural operation.

- For CI concepts, the rule induction is strictly object-centric and focus on object-level appearance

abstraction. The textual instruction \mathcal{T}^{sem} provides the semantic anchor, while the reference objects $\{o_i\}_{i=1}^N$ from visual references $\mathcal{R} = \{v_i\}_{i=1}^N$ provide appearance evidence of the target concept. Under this demand, the induced rule should emphasize the shared intrinsic appearance of the target objects:

$$\eta_{\text{CI}} = \Psi_{\text{CI}}(\mathcal{R}, \mathcal{T}^{\text{sem}}) \rightsquigarrow \mathcal{T}^{\text{sem}} \leftrightarrow \{o_i\}_{i=1}^N \quad (17)$$

- For CD concepts, the rule induction shifts from isolated object appearance to intra-sample contextual abstraction. The semantic instruction \mathcal{T}^{sem} acts as a relational query that specifies the contextual pattern to be identified. Under this demand, the induced rule should capture how the target foreground o_i is defined through its interaction with the environmental context C_{o_i} , and distill the invariant contextual dependency across references:

$$\eta_{\text{CD}} = \Psi_{\text{CD}}(\mathcal{R}, \mathcal{T}^{\text{sem}}) \rightsquigarrow \mathcal{T}^{\text{sem}} \leftrightarrow \{o_i \leftrightarrow C_{o_i}\}_{i=1}^N \quad (18)$$

- For CR concepts, the rule induction further shifts toward complex relational rule deduction across the entire reference set. The reasoning instruction \mathcal{T}^{rea} specifies the task demand and conceptual premise of the target rule. Under this demand, the induced rule should be derived from the joint interpretation of the reasoning instruction and the available visual references $\{v_i\}_{i=1}^N$:

$$\eta_{\text{CR}} = \Psi_{\text{CR}}(\mathcal{R}, \mathcal{T}^{\text{rea}}) \rightsquigarrow \mathcal{T}^{\text{rea}} \leftrightarrow (v_1 \leftrightarrow v_2 \leftrightarrow \dots \leftrightarrow v_N) \quad (19)$$

When multiple visual references are available, this rule induction may involve inter-sample relational reasoning aligned with the reasoning instruction. When only a single reference image is available, the inter-sample relation naturally degenerates, and the rule is constructed primarily from the text-defined reasoning premise while being grounded by the available visual evidence.

This framework explains how the identical cross-modal architecture can adapt its rule induction behavior under different concept complexities. It shifts fluidly from object-level appearance abstraction (CI), to intra-sample contextual abstraction (CD), and ultimately to complex relational rule deduction (CR), thereby supporting a unified modeling of highly heterogeneous concept categories.

A.6 Visualizing Dependency and Reasoning Conditions

CI concepts, such as people, vehicles, or ships, are relatively stable and environment-invariant, making their identities straightforward to determine from intrinsic appearance alone. In contrast, CD or CR concepts require additional forms of dependency beyond object identity. As shown in Fig. 6, several representative CD and CR concepts are illustrated together with the conditions that distinguish them as different concept categories. CD concepts primarily rely on foreground-background dependence, where the target’s visibility and concept identity are determined by its relationship to the surrounding context. For instance, camouflage is defined by visual similarity between the target and its background, transparency depends on background refraction and scene composition, industrial anomalies are determined through comparison with the structural regularity of the product body, and medical lesions become identifiable only under imaging conditions relative to surrounding healthy tissue. These examples demonstrate that CD targets often lack clear semantic meaning in isolation and can be reliably identified only through contextual contrast. CR concepts require multi-hop reasoning across entities, relations, and attributes. Identification is achieved through a sequential inference process that integrates visual and textual cues. For instance, locating a “pure black dog sitting under the tree” requires first grounding the tree, establishing the spatial relation “under”, and then filtering by the attribute “pure black”. Similarly, tasks such as logical compatibility, functional equivalence, or temporal consistency depend on reasoning over relationships rather than visual contrast alone.

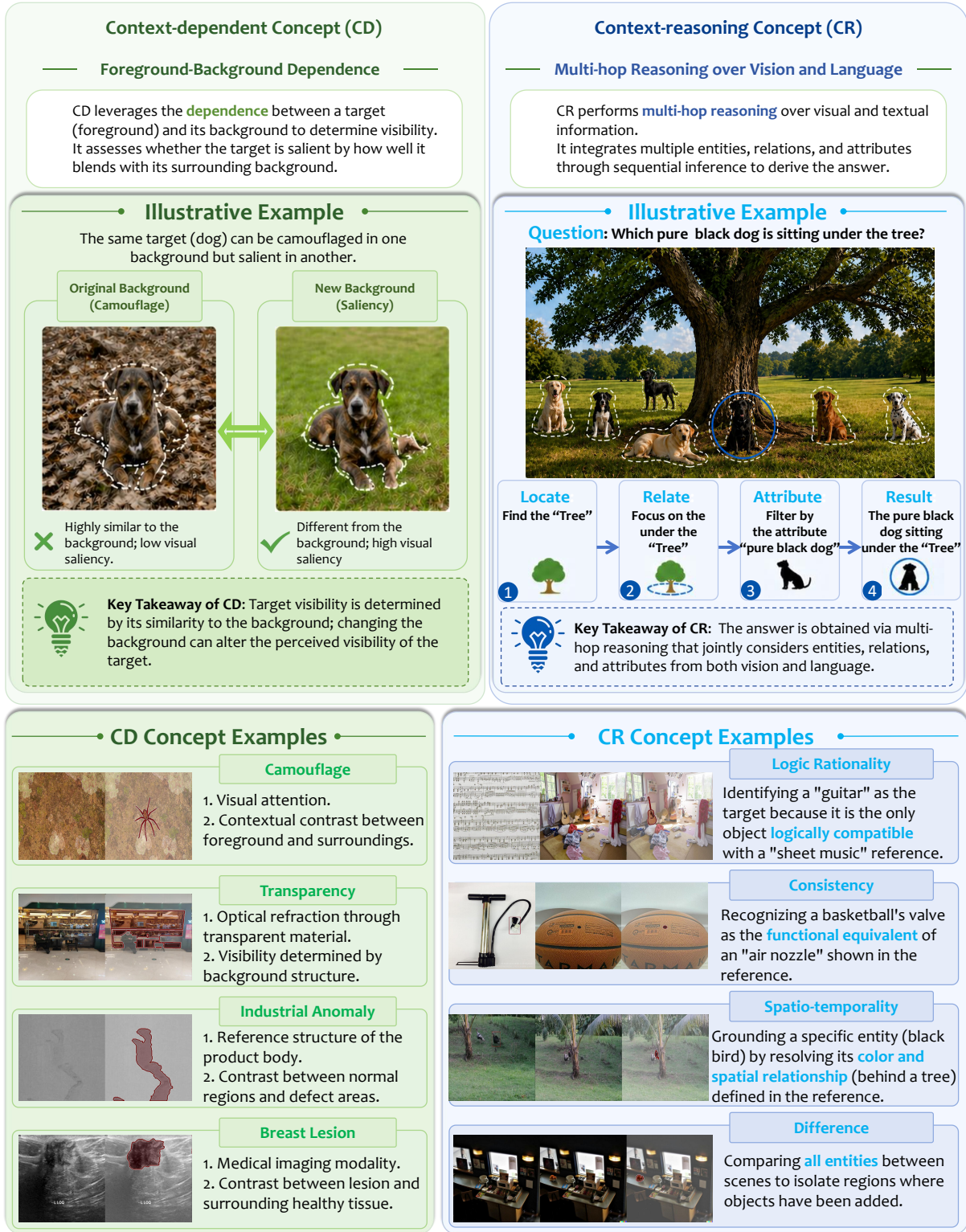


Figure 6. Visual comparison between CD and CR Concepts.

B Hierarchical Concept Segmentation Benchmark Suite

We curate a hierarchical concept segmentation benchmark suite to evaluate the out-of-distribution generalization of ConceptSeg-R1 across CI, CD, and CR concepts. As summarized in Tab. 5, this suite integrates a series of existing benchmarks and is organized into a training split for rule induction and an evaluation split structured according to the proposed CI/CD/CR taxonomy.

Table 5. Concept segmentation dataset overview. “*” denotes re-organized or modified datasets (§ B).

	Concept	Dataset	#Images	Description
Training Split (Total: 42,860 images)				
CD	Saliency	DUTS-TR [36]	10,548	Large-scale salient object, diverse natural scenes
	Camouflage	COD10K-TR [37]	4,040	Camouflaged animals/objects in natural habitats
CR	Consistency	FSS-1000R [38]	10,000	Few-shot segmentation, diverse object classes
		MGrounding* [39]	9,102	Reasoning to identify co-existing objects across images
	CoSOD3K [40]	3,316	Co-salient objects in relevant image groups	
	Difference	MGrounding* [39]	5,854	Reasoning to identify distinct objects between images
Evaluation Benchmark (Total: 29,696 images)				
CI	Living Classes	COCO20i* [41]	1,700 (17 Classes)	Common living object classes for base segmentation
	Artifact Classes	COCO20i* [41]	6,244 (63 Classes)	Man-made artifact categories in complex scenes
	Fine-grained Classes	iNaturalist* [6]	5,325 (2,537 Classes)	Fine-grained species recognition localization
	Ultra Rare Classes	iNaturalist* [6]	52 (26 Classes)	Long-tail distribution, extremely rare species
CD	Optical Property (Transparency)	Trans10K [42]	4,428	Transparent object segmentation in real scenes
	Optical Property (Shadow)	SBU [43]	638	Shadow detection and reflection surface analysis
	Camouflage	COD10K-TE [37]	2,026	Held-out camouflaged object evaluation split
	Saliency	DUTS-TE [36]	5,017	Standard salient object detection test split
	Industrial Anomaly	ESDIs-SOD* [44]	717 (12 classes)	Surface defects in diverse industrial materials
	Polyp Lesion	Colon Polyp [45]	798	Clinical colonoscopy images for polyp detection
	Breast Lesion	BUSI [46]	161	Breast Ultrasound images (Normal, Benign, Malignant)
	Skin Lesion	ISIC18 [47]	808	Skin lesion analysis and dermoscopy segmentation
	Common Consistency	MIG* [39]	477	Identify shared concepts among diverse images
	Correspondence Consistency	MIG* [39]	84	Semantic matching and pixel-level correspondence
CR	Reference Consistency	MIG* [39]	93	Locate targets based on specific reference prompts
	Static Difference	MIG* [39]	187	Discriminate varied objects from reference set
	View Difference	MIG* [39]	85	Identify changes across different viewpoints
	Logical Rationality	MIG* [39]	89	High-level logical inference and attribute mapping
	Cross-View Spatio-temporality	MIG* [39]	224	Consistency across multi-angle scene captures
	Cross-Frame Spatio-temporality	MIG* [39]	543	Dynamic reasoning for temporal object persistence

Table 6. Additional evaluation benchmarks. Generic segmentation benchmarks evaluate whether ConceptSeg-R1 preserves the native segmentation capability inherited from SAM 3, while reasoning-oriented benchmarks assess external reasoning-grounded segmentation ability.

Concept	Task	Dataset	#Images	Purpose
CI	Urban Scene Semantic Segmentation	Cityscapes [22]	500 (19 Classes)	Scene-level robustness
CR	Reasoning Segmentation	ReasonSeg-Val [17]	200	Evaluation of basic reasoning logic
		ReasonSeg-Test [17]	779	Intricate reasoning and world knowledge

In addition, we introduce supplementary evaluation benchmarks in Tab. 6.

Training Sets. The training split focuses on CD and CR concepts, since SAM 3 already provides strong native capability for many CI concepts. For CD concepts, we use salient object detection and camouflaged object detection as a reciprocal pair to strengthen foreground-background contrast perception. For CR concepts, we use consistency reasoning and difference reasoning datasets to encourage the model to distinguish shared patterns from discriminative variations across images. This design encourages ConceptSeg-R1 to learn transferable rules while preserving the inherent segmentation ability of the SAM 3 backbone.

Dataset Reconstruction. We detail the reconstruction and modification of existing datasets (“*” in Tab. 5) to construct our benchmark:

- COCO20i [41]: We manually partition data classes into *Artifact and Living Classes*. For each class, we randomly sample up to 100 images. For the classes with fewer than 100 images, all available samples are included.
- iNaturalist [6]: Classes are stratified into *Fine-grained and Ultra Rare Classes* based on SAM 3’s prediction confidence. The bottom 1% of classes by confidence are designated as Ultra Rare. For each class, we sample 10% of the images, ensuring a minimum of two images per class.
- ESDIs-SOD [44]: We preserve most classes with precise annotations and discard the 3rd and 5th classes due to their diffuse and loosely distributed labeled areas, which do not meet our quality standards.

- MGrounding [39]: We repurpose the MGrounding dataset by elevating its bounding box annotations to pixel-level masks via SAM 3.
- MIG [39]: Based on the multi-task grounding framework in MIG, we convert bounding boxes into high-quality masks via SAM 3 and manually filter out low-quality samples. A rigorous manual audit was conducted to prune instances with ambiguous boundaries or low-quality masks, ensuring a clean and dense supervision signal for the concept query learning. To construct our reasoning-heavy benchmark, we systematically adapted the original MIG grounding tasks into eight segmentation sub-tasks:
 1. *Common Consistency* from Common Object Grounding;
 2. *Correspondence Consistency* from Correspondence Grounding;
 3. *Reference Consistency* from Referring Grounding;
 4. *Static Difference* from Static Difference Grounding;
 5. *View Difference* from View Difference Grounding;
 6. *Logical Rationality* from Reasoning Grounding;
 7. *Cross-View Spatio-temporality* from Multi-View Grounding;
 8. *Cross-Frame Spatio-temporality* from Object Tracking.

Evaluation Benchmark. The main evaluation benchmark in Tab. 5 is organized into three levels of cognitive complexity to decouple intrinsic recognition from context-aware and reasoning-intensive segmentation. CI concept segmentation tasks evaluate appearance-driven recognition, including common classes, artifact classes, fine-grained classes, and ultra-rare long-tail concepts. CD concept segmentation tasks evaluate optical properties, camouflage, saliency, industrial anomalies, and medical lesions, where targets are defined by their relations to the environment. CR concept segmentation tasks evaluate multi-step visual-textual reasoning, including consistency, difference, logical rationality, and spatio-temporality, requiring cross-image dependencies or higher-order relational understanding. This hierarchy provides a unified protocol for assessing generalized concept segmentation across perception, contextual understanding, and reasoning.

Supplementary Evaluation. As shown in Tab. 6, we further introduce several external benchmarks to provide a broader evaluation of ConceptSeg-R1. These benchmarks can still be interpreted within our concept framework, but we report them in their original benchmark form rather than further subdividing them by concept category, so as to examine performance preservation and facilitate comparison with existing methods under existing used evaluation protocols. Specifically, in Tab. 2, we evaluate the model on Cityscapes [22], a generic segmentation benchmark that conforms to our CI concept definition, as its semantic categories are primarily determined by stable visual semantics. This evaluation verifies that reasoning-oriented training does not compromise the general-purpose, CI-style segmentation ability inherited from SAM 3. We also include ReasonSeg-Val/Test [17] as an external reasoning-grounded segmentation benchmark in Tab. 3. ReasonSeg mainly evaluates single-image reasoning-grounded segmentation with textual instructions, and can be viewed as a CR-style evaluation closely related to logical rationality.

C Implementation Details

Our training process consists of two primary stages: supervised fine-tuning for alignment and cognitive reinforcement learning for reasoning optimization. All experiments are conducted using the AdamW [48] optimizer with a linear learning rate scheduler, where reference and reasoning images are uniformly resized to 600×600 pixels. To ensure reproducibility, the random seed is fixed at 42.

Table 7. Hyper-parameters configuration.

(a) Stage 1: Supervised Fine-Tuning.		(b) Stage 2: Cognitive Fine-Tuning.	
Configuration	Value	Configuration	Value
Training Epochs	20	Training Epochs	2
Batch Size	128	Batch Size	64
SAM 3 Image Size	1008×1008	SAM 3 Image Size	1008×1008
Learning Rate	3×10^{-5}	Learning Rate	1×10^{-6}
Optimizer	AdamW	Optimizer	AdamW
Learning Rate Scheduler	Linear	Learning Rate Scheduler	Linear
Max Prompt Length	2048	Max Prompt Length	2048
Max Completion Length	768	Max Completion Length	768
Concept Query Length (L_2)	8	Concept Query Length (L_2)	8
GRPO Beta (β)	0.04	GRPO Beta (β)	0.04
Trainable Parameters	CTM	Trainable Parameters	MLLM, CTM
Random Seed	42	Random Seed	42

C.1 Stage 1: Supervised Fine-Tuning

In the first stage, we focus on aligning the multi-modal reasoning capabilities with the concept translation module (CTM). We employ an image resolution of 1008×1008 for the SAM 3 backbone and 600×600 for reference images. During this stage, only the parameters of the CTM are updated. Detailed hyper-parameters are provided in Tab. 7a.

C.2 Stage 2: Cognitive Reinforcement Learning

In the second stage, we utilize Meta-GRPO to enhance the model’s deductive reasoning and rule-following abilities. The learning rate is reduced to 1×10^{-6} to maintain training stability. We jointly optimize the MLLM and the CTM. For each prompt, we sample a group of $G = 8$ outputs to calculate the relative advantage within GRPO. The detailed configurations are summarized in Tab. 7b.

D Prompt Templates

In this section, we detail the structured prompt templates employed in ConceptSeg-R1. To bridge the gap between low-level visual features and high-level conceptual reasoning, we adopt a hierarchical instruction format that organizes input signals into *Support*, *Proxy*, and *Query* components.

D.1 Standard Instruction Template

Our template is designed to elicit explicit chain-of-thought (CoT) rationales before generating spatial coordinates. The system prompt enforces a strict rule-induction protocol, requiring the model to verify induced rules on a specific sub-region (the “Check” step) before finalizing the target localization.

System Prompt & Template

Instruction: Your task is to locate the object matching problem in the target image.

Reference Image: Bounding boxes provided at reference_boxes.

Target Image: The image for grounding.

Protocol: Think through the reasoning process in your mind, induce the visual rule and check it by locating the missed bounding box in the reference image, apply this rule to locate the corresponding object in the Target Image.

Output strictly in the following format: `<think>[Your step-by-step analysis and reasoning]</think>`
`<rule>Visual rule of the reference targets</rule>` `<check>[x1, y1, x2, y2]</check>` `<bbox>[x3, y3, x4, y4]</bbox>` `<answer>concise noun phrase for target object</answer>`

D.2 Token Representations and Semantic Placeholders

To ensure the multi-modal large language model (MLLM) correctly interprets the input data, we define the following special tokens and placeholders:

- [problem]: A natural language query or conceptual description (e.g., “the most fragile object”).
- [reference_boxes]: Normalized coordinates $[x_{min}, y_{min}, x_{max}, y_{max}]$ representing the *Support* set targets.
- <think>: Dedicated tags for the Reasoning-Chain (CoT), incentivized via GRPO to perform rule induction.
- <rule>: A concise linguistic abstraction representing the relational mapping between the reference and target images. It encapsulates the underlying logic of the task (e.g., identity, difference, or functional scaling).
- <check>: A diagnostic bounding box used to verify the induced rule on the reference image’s “proxy query”.
- <bbox>: The final predicted coordinates for the Target Image.
- <answer>: A brief, 1-3 word noun phrase identifying the segmented concept to ensure linguistic grounding, which are subsequently passed to the Segment Anything Model (SAM 3).

D.3 Compositional Sensitivity and Mosaic Processing

The template is highly adaptive to various input configurations and data augmentations:

- **Support/Proxy Scaling (K^2 -shot):** The template dynamically accommodates K^2 support samples. As K increases, the [reference_boxes] list expands, facilitating complex cross-instance comparisons.
- **Reference Image Mosaic Strategy:** To handle multi-image context within a fixed window, reference images are organized into a $K \times K$ mosaic. Each image is resized to a specific sub-region (e.g., 1/2 size for a 2×2 grid). Original masks and bounding box coordinates undergo a corresponding scale transformation to fit the new mosaic layout.
- **Global Coordinate Normalization:** All spatial coordinates within the template are globally normalized relative to the entire mosaic canvas. This ensures a consistent spatial reference frame for rule induction and proxy verification across diverse aspect ratios.
- **Proxy Query Presence:** The template facilitates toggling the “Proxy Query” (i.e., the intentionally omitted bounding box in the reference image). When activated, it functions as an intermediate reasoning anchor for rule verification. In single-reference scenarios, the model directly induces the task rule and proceeds to localize the target object.

E Comprehensive Quantitative Results

In this section, we provide a comprehensive performance comparison between ConceptSeg-R1 and existing methods.

Metrics: Beyond the metrics discussed in the main text, we introduce four additional evaluation metrics: Mean Absolute Error (MAE), Balance Error Rate (BER), S-measure (S_m), and Mean Dice (mDice). These metrics validate the superior performance of ConceptSeg-R1 across multiple

Table 8. Per-dataset results and mean performance.

Metric	CI Concepts				CD Concepts										CR Concepts									
	Living Classes	Artifact Classes	Fine-grained Classes	Ultra Rare Classes	Optical Property		Camouflage	Saliency	Industrial Anomaly	Polyp Lesion	Breast Lesion	Skin Lesion	Consistency			Difference		Rationality	Spatio-temporality					
	COCO20s	COCO20s	iNaturalist	iNaturalist	Mean	SBU	Trans10K	COD10KTE	DUTS-TE	ESDy-SOD	Colon Polyp	BUSI	ISIC18	Mean	Common	Correspondence	Reference	Static	View	Logical	View	Frame	Mean	
SAM 3 [6]																								
MAE ↓	2.20	1.98	0.50	0.57	1.31	6.10	3.75	23.55	16.43	10.55	24.88	12.01	50.53	18.48	-	-	-	-	-	-	-	-	-	-
BER ↓	6.37	7.93	1.70	1.87	4.47	13.03	4.60	23.32	32.19	22.79	36.26	21.91	37.99	24.01	-	-	-	-	-	-	-	-	-	-
F_{β}^{\uparrow}	86.28	80.11	96.03	95.72	89.54	79.67	91.46	51.28	38.06	51.48	17.46	49.57	41.86	52.60	-	-	-	-	-	-	-	-	-	-
$S_m \uparrow$	87.73	82.14	93.50	95.91	89.82	79.30	91.23	62.59	58.46	66.22	45.50	67.35	37.00	63.46	-	-	-	-	-	-	-	-	-	-
mIoU ↑	88.66	85.40	96.74	96.47	91.82	81.49	91.34	61.43	58.97	66.17	44.91	65.53	36.31	63.27	-	-	-	-	-	-	-	-	-	-
mDice ↑	87.23	81.58	96.07	95.86	90.19	80.70	92.87	54.44	39.70	53.11	21.61	53.79	48.34	55.57	-	-	-	-	-	-	-	-	-	-
LENS-3B [16]																								
MAE ↓	6.49	4.16	1.23	0.96	3.21	15.25	14.80	6.17	6.08	19.47	10.58	9.23	13.35	11.87	20.07	10.36	8.33	14.01	5.89	6.90	4.92	3.12	9.20	9.20
BER ↓	16.86	17.00	2.49	2.32	9.67	32.33	18.25	18.74	12.98	32.45	20.45	23.37	13.60	21.52	40.14	29.65	33.31	35.60	32.53	40.86	37.01	14.88	33.00	33.00
F_{β}^{\uparrow}	64.18	55.70	89.98	87.74	74.40	43.20	68.88	58.08	76.90	51.34	49.91	44.08	73.91	58.29	28.41	20.87	30.77	22.28	28.98	19.52	25.73	61.61	29.77	29.77
$S_m \uparrow$	73.94	71.81	92.23	90.83	82.20	58.15	72.46	73.15	81.72	61.38	68.78	65.12	76.63	69.67	48.64	53.93	58.94	52.17	59.93	53.54	58.07	77.82	57.88	57.88
mIoU ↑	74.29	72.51	92.39	91.71	82.73	58.85	71.91	73.08	81.05	60.17	67.72	65.00	74.68	69.06	51.08	54.43	60.04	53.10	60.43	55.08	58.76	77.63	58.82	58.82
mDice ↑	65.58	57.98	91.43	89.17	76.04	43.90	70.24	60.42	77.35	50.38	53.42	48.55	75.24	59.91	28.18	24.01	32.52	24.88	30.60	20.52	26.85	64.12	31.46	31.46
Seg-Zero-7B [15]																								
MAE ↓	2.91	2.57	0.62	0.49	1.65	13.50	9.31	5.89	10.58	26.92	15.32	8.00	12.00	12.69	23.53	7.86	8.17	7.63	3.67	9.17	6.13	7.99	9.27	9.27
BER ↓	7.99	10.57	1.97	1.39	5.48	26.32	10.25	11.35	9.49	28.39	20.82	19.94	19.12	18.21	43.47	44.71	42.99	46.42	48.83	46.11	47.37	48.23	46.02	46.02
F_{β}^{\uparrow}	82.80	73.28	95.10	96.03	86.80	54.33	79.81	74.95	72.76	51.43	51.18	56.24	73.31	64.25	22.25	7.20	18.89	9.32	1.72	9.80	7.50	6.80	10.44	10.44
$S_m \uparrow$	85.62	79.19	95.31	93.58	88.43	63.33	81.54	82.06	80.26	58.02	67.27	71.64	75.20	72.44	43.96	47.47	52.34	47.79	47.16	47.28	48.03	46.95	47.70	47.70
mIoU ↑	86.29	81.63	95.91	96.47	90.08	65.00	81.21	81.11	78.56	57.12	65.72	70.07	73.07	71.56	45.74	49.19	53.89	49.54	48.78	49.29	49.01	48.79	49.37	49.37
mDice ↑	83.81	75.18	95.46	96.31	87.69	56.05	82.95	76.82	76.34	52.36	54.29	59.77	72.80	66.42	24.45	8.09	19.50	9.97	2.17	10.64	7.89	7.26	11.25	11.25
SAM3-Agent-3B [6]																								
MAE ↓	7.33	5.98	4.83	2.78	5.23	16.22	16.75	11.52	9.61	17.19	14.84	23.57	51.88	20.20	16.47	4.69	3.32	4.82	3.37	6.96	2.01	5.41	5.88	5.88
BER ↓	26.56	33.89	17.40	13.21	22.77	33.48	24.57	29.37	23.35	45.22	46.66	41.40	58.46	37.81	34.68	18.99	30.53	29.55	32.22	31.48	21.13	44.23	30.35	30.35
F_{β}^{\uparrow}	45.11	34.53	66.11	74.84	55.15	40.80	54.17	45.36	59.47	20.59	10.06	19.92	21.23	33.95	25.78	1.18	34.00	1.44	3.70	20.28	9.76	10.54	13.46	13.46
$S_m \uparrow$	62.60	61.68	77.84	84.30	71.61	57.62	65.94	64.91	72.08	49.20	47.24	46.71	25.40	53.64	50.13	17.35	60.90	28.15	33.91	46.40	28.84	50.82	39.56	39.56
mIoU ↑	62.51	62.05	79.91	84.92	72.35	58.22	63.75	64.76	72.07	49.14	47.03	46.28	30.95	54.30	50.66	17.75	61.04	28.03	33.81	46.90	29.03	51.92	39.89	39.89
mDice ↑	44.82	34.38	65.89	74.67	54.94	40.98	55.03	45.87	59.08	19.12	10.39	21.04	22.78	34.29	25.95	1.48	33.94	1.38	4.53	20.48	9.75	11.20	13.59	13.59
SAM3-Agent-7B [6]																								
MAE ↓	4.44	3.35	0.98	0.97	2.44	10.09	10.64	10.20	7.75	22.64	20.94	25.67	57.19	20.64	9.43	2.65	3.15	5.63	2.82	3.75	0.71	7.22	4.42	4.42
BER ↓	18.69	20.96	7.26	4.73	12.91	23.66	13.98	23.32	16.03	40.25	45.07	35.83	61.10	32.53	19.24	20.78	31.45	28.37	31.34	28.62	12.19	38.22	26.28	26.28
F_{β}^{\uparrow}	68.32	60.60	86.31	91.79	76.76	61.33	75.21	58.86	74.43	31.45	17.30	32.48	25.50	47.07	47.39	1.38	31.37	25.05	28.29	29.25	13.76	13.16	23.71	23.71
$S_m \uparrow$	77.23	73.45	88.72	93.36	83.19	68.84	78.69	71.79	80.10	48.85	47.13	51.15	22.64	58.59	59.24	19.97	59.78	48.52	56.63	52.78	23.35	49.51	46.22	46.22
mIoU ↑	77.46	74.98	91.61	94.11	84.54	70.25	78.44	71.65	80.20	49.03	46.91	50.70	29.93	59.64	60.00	20.62	59.89	48.87	57.39	53.26	23.90	50.29	46.78	46.78
mDice ↑	67.88	60.56	86.20	91.58	76.56	60.99	76.44	59.25	74.04	30.36	17.97	33.42	26.88	47.42	47.65	1.65	31.44	25.35	28.37	29.03	13.54	15.01	24.01	24.01
ConceptSeg-R1-3B																								
MAE ↓	2.27	2.17	0.40	0.49	1.33	6.10	3.73	2.52	4.18	10.97	6.37	6.93	8.36	6.15	5.87	11.41	1.99	9.95	2.36	6.55	4.31	1.35	5.47	5.47
BER ↓	6.38	8.13	1.03	1.63	4.29	13.03	4.60	6.98	4.66	18.28	16.60	14.82	10.63	11.20	9.92	18.33	10.14	21.24	19.66	28.06	26.93	5.84	17.52	17.52
F_{β}^{\uparrow}	86.17	79.93	96.92	96.45	89.87	79.82	91.57	83.65	88.96	61.52	58.96	66.75	81.14	76.55	80.11	34.59	77.07	49.68	55.78	46.57	49.90	79.51	59.15	59.15
$S_m \uparrow$	87.52	81.80	93.65	96.07	89.76	79.22	91.12	88.19	90.80	71.59	75.09	77.54	82.96	82.06	84.80	60.03	85.53	67.34	73.14	67.49	69.62	87.49	74.43	74.43
mIoU ↑	88.55	85.20	97.38	96.87	92.00	81.56	91.37	87.65	90.47	70.97	74.31	76.33	81.50	81.77	85.77	59.69	85.57	68.21	75.41	68.49	70.24	88.05	75.18	75.18
mDice ↑	87.09	81.36	97.16	96.61	90.56	80.84	92.94	84.87	89.74	62.57	61.40	69.92	81.55	77.98	81.39	38.67	78.24	51.85	56.80	47.03	49.95	81.83	60.72	60.72
ConceptSeg-R1-7B																								
MAE ↓	2.17	2.19	0.39	0.43	1.30	6.06	3.74	2.18	1.92	9.35	6.11	5.87	7.58	5.35	4.80	5.23	1.65	3.97	2.18	3.22	3.01	1.01	3.13	3.13
BER ↓	6.46	8.68	0.98	1.09	4.30	13.00	4.61	6.93	2.78	17.59	15.10	15.42	10.40	10.73	8.23	19.47	11.10	16.26	24.33	19.38	21.79	5.48	15.82	15.82
F_{β}^{\uparrow}	86.86	79.39	96.56	96.76	89.89	79.84	91.57	84.75	92.65	66.67	65.01	69.56	82.22	79.03	83.42	49.81	77.13	64.98	48.99	60.22	58.12	81.39	65.51	65.51
$S_m \uparrow$	87.63	81.73	96.05	93.62	89.76	79.22	91.11	88.75	93.65	74.47	78.50	79.39	83.93	83.63	86.99	68.03	85.25	76.41	70.18	76.27	73.96	88.75	78.23	78.23
mIoU ↑	88.77	85.32	97.19	97.24	92.13	81.57	91.37	88.28	93.53	74.10	77.20	78.17	82.48	83.34	87.87	69.60	85.53	77.80	72.12	76.69	74.47	89.14	79.15	79.15
mDice ↑	87.18	80.76	96.88	96.99	90.45	80.85	92.94	85.76	93.19	67.04	66.57	71.31	82.63	80.04	84.71	52.03	77.72	65.92	49.48	61.56	58.68	83.02	66.64	66.64

Table 9. Ablation study of reward components in ConceptSeg-R1-3B. Results are averaged over all concepts in CI, CD, and CR under all evaluation metrics.

Method	CI Concepts				CD Concepts				CR Concepts			
	MAE ↓	BER ↓	F_{β}^{\uparrow}	$S_m \uparrow$	mIoU ↑	mDice ↑	MAE ↓	BER ↓				

Table 10. Ablation study of Shortcut Router between SAM 3 and the reasoning branch in ConceptSeg-R1-3B. The routing rate denotes the proportion of samples directly processed by SAM 3.

Concept	Routing Rate (%)	$F_{\beta}^w \uparrow$				mIoU \uparrow			
		SAM 3 Only	Full Reasoning	Adaptive Reasoning	Δ Gains	SAM 3 Only	Full Reasoning	Adaptive Reasoning	Δ Gains
<i>CI Concepts</i>									
Living Classes	97.60	86.28	72.45	86.17	+13.72	88.66	80.54	88.55	+08.01
Artifact Classes	96.10	80.11	61.91	79.93	+18.02	85.40	75.56	85.20	+09.64
Fine-grained Classes	86.50	96.03	96.65	96.92	+00.27	96.74	97.24	97.38	+00.14
Ultra Rare Classes	7.70	95.72	95.58	96.45	+00.87	96.47	96.37	96.87	+00.50
<i>CD Concepts</i>									
Optical Property (Shadow)	99.50	79.67	43.45	79.82	+36.37	81.49	58.50	81.56	+23.06
Optical Property (Transparency)	99.90	91.46	69.70	91.57	+21.87	91.34	74.37	91.37	+17.00
Camouflage	8.40	51.28	83.94	83.65	-00.29	61.43	87.96	87.65	-00.31
Saliency	0.00	38.06	88.96	88.96	0.00	58.97	90.47	90.47	0.00
Industrial Anomaly	0.00	51.48	61.52	61.52	0.00	66.17	70.97	70.97	0.00
Polyp Lesion	0.00	17.46	58.96	58.96	0.00	44.91	74.31	74.31	0.00
Breast Lesion	0.70	49.57	66.90	66.75	-00.15	65.53	76.52	76.33	-00.19
Skin Lesion	0.00	41.86	81.14	81.14	0.00	36.31	81.50	81.50	0.00
<i>CR Concepts</i>									
Common Consistency	0.00	-	80.11	80.11	0.00	-	85.77	85.77	0.00
Correspondence Consistency	0.00	-	34.59	34.59	0.00	-	59.69	59.69	0.00
Reference Consistency	0.00	-	77.07	77.07	0.00	-	85.57	85.57	0.00
Static Difference	0.00	-	49.68	49.68	0.00	-	68.21	68.21	0.00
View Difference	0.00	-	55.78	55.78	0.00	-	75.41	75.41	0.00
Logical Rationality	0.00	-	46.57	46.57	0.00	-	68.49	68.49	0.00
Cross-View Spatio-temporality	0.00	-	49.90	49.90	0.00	-	70.24	70.24	0.00
Cross-Frame Spatio-temporality	0.00	-	79.51	79.51	0.00	-	88.05	88.05	0.00

F Reward Configuration Evaluation

We conduct reward ablation experiments to analyze the contribution of different reward components in ConceptSeg-R1-3B, including mask reward, box reward, and meta reasoning reward. As shown in Tab. 9, removing either the box & meta reward or the mask reward consistently degrades performance across CI, CD, and CR concepts. Among all settings, the full reward formulation achieves the best overall performance on nearly all metrics. In particular, removing the box and meta reward leads to a significant performance drop on CR concepts, indicating that structural grounding and reasoning-aware supervision are critical for complex reasoning segmentation. Meanwhile, removing the mask reward mainly affects CI and CD concepts, demonstrating the importance of pixel-level spatial supervision for perception-oriented segmentation. These results suggest that the different reward components provide complementary optimization signals, jointly improving spatial accuracy, structural consistency, and reasoning correctness in generalized concept segmentation.

G Routing Strategy Evaluation

In Tab. 10, we compare three routing strategies: always using the direct SAM 3 segmentation pathway (SAM 3 only), always executing the full reasoning pipeline (Full Reasoning), and the proposed adaptive routing strategy (Adaptive Reasoning). The results demonstrate that adaptive routing effectively balances efficiency and reasoning capability across different concept regimes. On CI concepts, where strong reasoning is unnecessary, the adaptive strategy achieves performance comparable to the direct SAM 3 pathway while consistently outperforming the full reasoning pipeline, indicating that the router preserves the native segmentation capability of SAM 3 without introducing unnecessary reasoning overhead. More importantly, the routing behavior adapts to task complexity within the CI regime. For relatively simple categories such as living and artifact classes, the routing rate remains above 95%, and the adaptive performance matches the direct SAM 3 results. In contrast, for more challenging categories such as fine-grained and ultra rare classes, an increasing portion of samples is routed to the reasoning branch. Specifically, on fine-grained classes, both “Full Reasoning” and “Adaptive Reasoning” outperform the “SAM 3 Only”, indicating the benefit of reasoning for subtle visual distinctions. On ultra rare classes, “Full Reasoning” alone slightly underperforms “SAM 3 Only”, whereas the proposed “Adaptive Reasoning” consistently achieves the best performance. These results demonstrate that the router dynamically balances perception and reasoning according to task

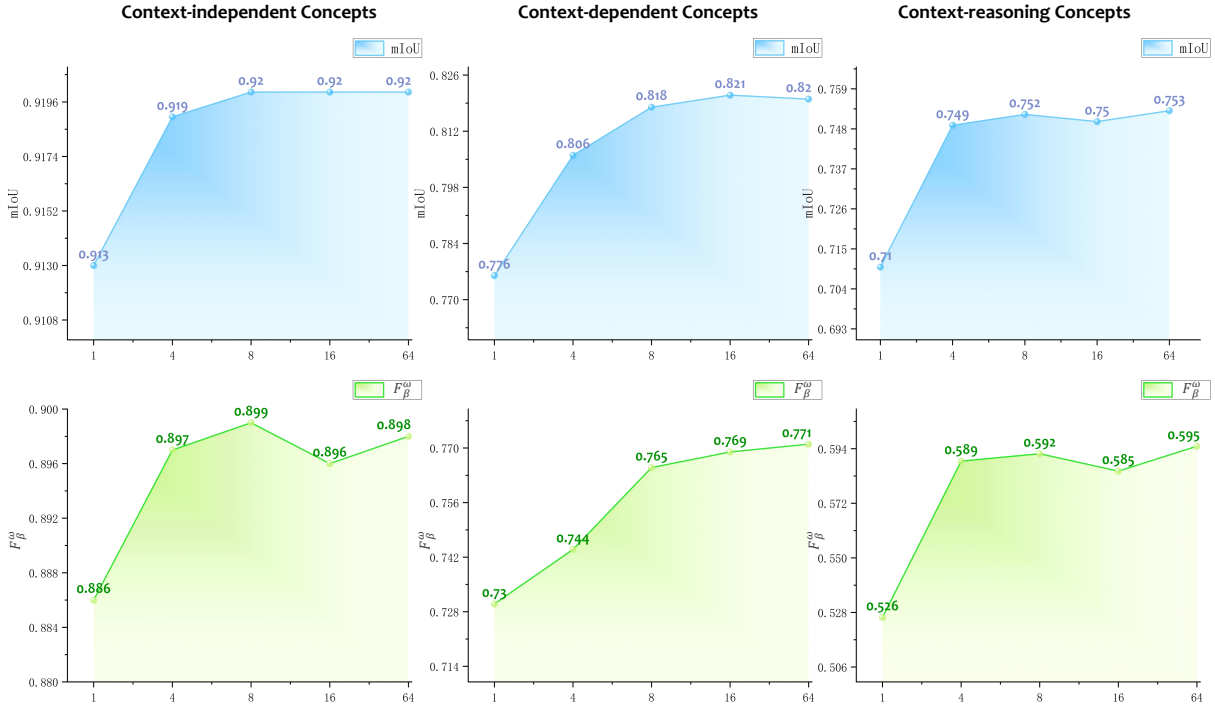


Figure 7. Impact of the concept query length (L_2) on concept segmentation benchmarks. Results for mIoU and F_β^ω are reported as dataset-level averages.

difficulty. On CD concepts, the adaptive strategy yields substantial improvements over always reasoning, particularly in shadow and transparency concepts, where gains of up to +0.23 mIoU are observed. A closer inspection reveals distinct routing patterns across different CD concept understanding tasks. For shadow and transparency concepts, the direct SAM 3 pathway already achieves strong performance and significantly outperforms the “Full Reasoning”, indicating that these tasks primarily depend on accurate visual perception rather than complex reasoning. In contrast, for other CD concepts, the “Full Reasoning” consistently surpasses the “SAM 3 Only”, demonstrating the necessity of contextual reasoning in these scenarios. Importantly, the proposed “Adaptive Reasoning” strategy learns to route samples accordingly: the routing rate approaches 100% for shadow and transparency concepts, while remaining near zero for other CD concepts. This behavior confirms that the router performs precise sample-level decision, activating reasoning only when beneficial and preserving direct perception when sufficient. On CR concepts, the routing rate consistently drops to zero, meaning that all samples are processed through the reasoning branch. This result validates that the router correctly identifies reasoning-intensive tasks and fully engages the reasoning pipeline when multi-step inference is necessary. Overall, these findings verify that the Shortcut Router enables dynamic allocation of computational resources, preserving efficiency on simple cases while maintaining strong reasoning performance on complex concept understanding tasks.

H Concept Query Sensitivity

We analyze the impact of varying the number of learnable concept queries (i.e., L_2 in $\mathbf{C} \in \mathbb{R}^{L_2 \times C}$ as stated in § 3.3 and equation (3)), to assess the module’s sensitivity to contextual information, as illustrated in Fig. 7. Our analysis reveals two key insights:

- **Semantic Bottleneck.** When $L_2 = 1$, performance across all concept segmentation benchmarks is markedly suboptimal. This degradation stems from a semantic bottleneck between reasoning and segmentation: a single query token is insufficient to encapsulate the high-dimensional

Table 11. Evaluation of ConceptSeg-R1 under different randomly sampled reference prompts (mean \pm std over three runs).

Concept	MAE \downarrow	BER \downarrow	F_{β}^{ω} \uparrow	S_m \uparrow	mIoU \uparrow	mDice \uparrow
CI	1.35 \pm 0.02	4.38 \pm 0.12	89.76 \pm 0.16	89.55 \pm 0.29	91.89 \pm 0.16	90.44 \pm 0.16
CD	6.06 \pm 0.12	11.19 \pm 0.01	76.30 \pm 0.35	81.94 \pm 0.18	81.75 \pm 0.03	77.86 \pm 0.17
CR	5.44 \pm 0.05	17.31 \pm 0.29	59.14 \pm 0.01	74.36 \pm 0.10	75.17 \pm 0.02	60.69 \pm 0.05

Table 12. Ablation experiments of different reference configurations (1×1 vs. 2×2).

Concept	Reference	MAE \downarrow	BER \downarrow	F_{β}^{ω} \uparrow	S_m \uparrow	mIoU \uparrow	mDice \uparrow
CI	1 \times 1	1.40	4.53	89.54	89.27	91.70	90.24
	2 \times 2	1.33	4.29	89.87	89.76	92.00	90.56
	Δ Gains	+0.07	+0.24	-0.33	-0.49	-0.30	-0.32
CD	1 \times 1	7.22	11.23	75.01	80.77	80.58	76.92
	2 \times 2	6.15	11.20	76.55	82.06	81.77	77.98
	Δ Gains	+1.07	+0.03	-1.54	-1.29	-1.19	-1.06
CR	Default	5.47	17.52	59.15	74.43	75.18	60.72

reasoning outputs from the MLLM, thereby failing to provide SAM 3 with effective guidance for pixel-level localization.

- **Robustness and Convergence.** As L_2 increases, we observe a consistent performance gain that converges at $L_2 = 8$. This trend suggests that the model is highly robust once the query length exceeds this threshold, as $L_2 \geq 8$ effectively alleviates the bottleneck by providing sufficient semantic bandwidth to convey refined prompt for SAM 3. Consequently, to maintain an optimal trade-off between computational efficiency and segmentation accuracy, we fix $L_2 = 8$ for our final configuration.

I Reference Robustness and Configuration

We evaluate the robustness of ConceptSeg-R1 under different reference prompts and analyzes the impact of reference configurations.

- **Random Reference Stability.** We first evaluate the stability of ConceptSeg-R1 using randomly sampled reference prompts across three independent runs with different random seeds. As shown in Tab. 11, the model achieves highly consistent performance across CI, CD, and CR concepts, with all standard deviations remaining very small under different metrics. Among the three concept regimes, CI concepts exhibit the highest stability, while CD and CR concepts also maintain robust performance despite involving more complex contextual dependency and reasoning processes. During training, the reference prompts are randomly composed from different support examples, forcing the model to induce transferable task rules rather than overfitting to fixed prompt layouts or specific instances. This randomized prompt composition improves robustness to diverse reference configurations and enhances generalization under varying prompt distributions. These results demonstrate that ConceptSeg-R1 is insensitive to specific reference selections and generalizes reliably across diverse prompt compositions.
- **Reference Configuration Ablation.** We further compare different reference configurations by evaluating a 1×1 single-reference setting and a 2×2 mosaic-reference setting. As reported in Tab. 12, the 2×2 configuration consistently outperforms the 1×1 setting on both CI and CD concepts across nearly all metrics. The performance improvement is especially significant on CD concepts, indicating that multiple references provide richer contextual diversity and stronger cross-image consistency for task rule induction. In contrast, single-reference prompts are more susceptible to ambiguity and stochastic bias, making it harder for the model to infer reliable task-level concepts. For CR concepts, we adopt the default reference configuration due to the stronger dependence on reasoning-oriented prompt composition.

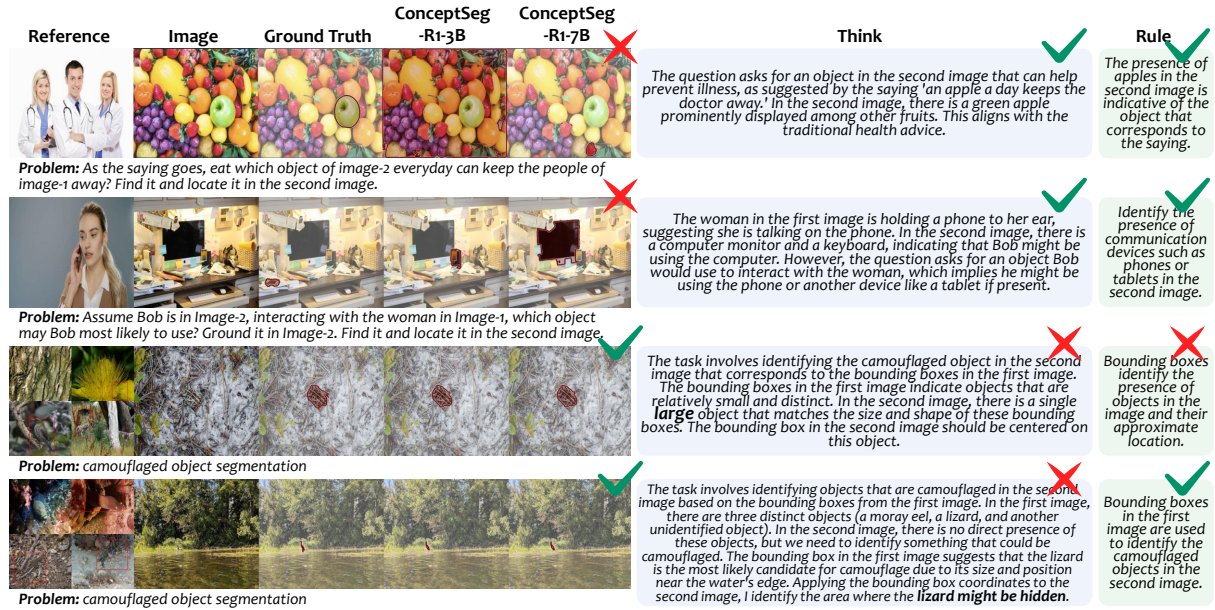


Figure 8. Visualization of the correctness relationships among segmentation prediction, reasoning trajectory (Think), and induced rule (Rule) in reasoning segmentation.

J Beyond Mask Accuracy: Decomposing Reasoning Segmentation

Existing reasoning-oriented segmentation benchmarks primarily evaluate the final segmentation mask, typically using overlap-based metrics such as mIoU or cIoU. However, a correct mask does not necessarily imply correct reasoning. A model may produce visually plausible predictions while relying on incorrect rules, spurious correlations, or shortcut reasoning paths. Therefore, evaluating only the final segmentation result is insufficient for understanding the true reasoning capability of concept segmentation systems.

To further analyze this issue, we provide a qualitative decomposition of the reasoning process in Fig. 8. Instead of evaluating only the final prediction, we explicitly examine the consistency among three components: the inferred reasoning trajectory (Think), the induced rule (Rule), and the final segmentation result (Prediction). Each component may independently succeed or fail, leading to different forms of reasoning correctness and failure cases. For example, a model may generate the correct segmentation mask while relying on incorrect reasoning logic, indicating shortcut learning rather than genuine concept understanding. Conversely, a model may induce semantically correct rules but fail during the final segmentation execution due to inaccurate grounding or imperfect mask decoding. These observations suggest that reasoning segmentation should be evaluated as a multi-stage process involving rule induction, reasoning consistency, grounding correctness, and final mask quality, rather than a single end-point prediction task. We hope this analysis can motivate future research toward more comprehensive evaluation protocols for reasoning segmentation, including intermediate reasoning supervision, rule consistency verification, and causal grounding assessment.

K Qualitative Visualization

We provide additional qualitative comparisons across CI, CD, and CR concepts, as shown in Figs. 9 to 14.

L Limitations and Future Works

As an initial step toward segmenting any concept, our ConceptSeg-R1 still presents several limitations and opportunities for future improvement. **I) Dependence on Representative Support Examples.** The effectiveness of rule induction relies on the quality and representativeness of the provided support examples. When support instances are highly ambiguous, visually noisy, or weakly aligned with the target concept, the inferred rule may be incomplete or suboptimal, potentially affecting downstream segmentation accuracy. Future work may address this limitation by incorporating automated support selection mechanisms, active example filtering, or confidence-aware retrieval strategies to improve the reliability of rule induction under challenging conditions. **II) Scalability to Extremely Long Reasoning Chains.** Current reasoning procedures are performed within a fixed context window and are primarily optimized for short to moderate reasoning sequences. Tasks requiring very long reasoning chains, complex temporal dependencies, or hierarchical multi-step planning may exceed the effective reasoning capacity of the current architecture. Future research could explore hierarchical reasoning structures, memory-augmented reasoning modules, or external reasoning buffers to support more scalable reasoning workflows. **III) Sensitivity to Routing Decisions in Dynamic Inference.** The shortcut routing mechanism improves efficiency by dynamically selecting between lightweight and full reasoning pipelines. However, incorrect routing decisions may occasionally lead to suboptimal performance, particularly when the input complexity lies near the boundary between concept categories. Future work may improve routing robustness through uncertainty-aware routing policies, adaptive threshold learning, or lightweight verification stages that reduce the impact of routing errors. **IV) Computational Overhead in Reasoning-Enhanced Segmentation.** Although ConceptSeg-R1 maintains practical inference latency, reasoning-enhanced segmentation generally introduces additional computational cost compared to purely feed-forward segmentation models. This overhead may become more pronounced in large-scale deployment scenarios or real-time applications with strict latency constraints. Future optimization efforts may focus on model compression, dynamic reasoning pruning, or hardware-aware scheduling to further improve computational efficiency while preserving reasoning capability.

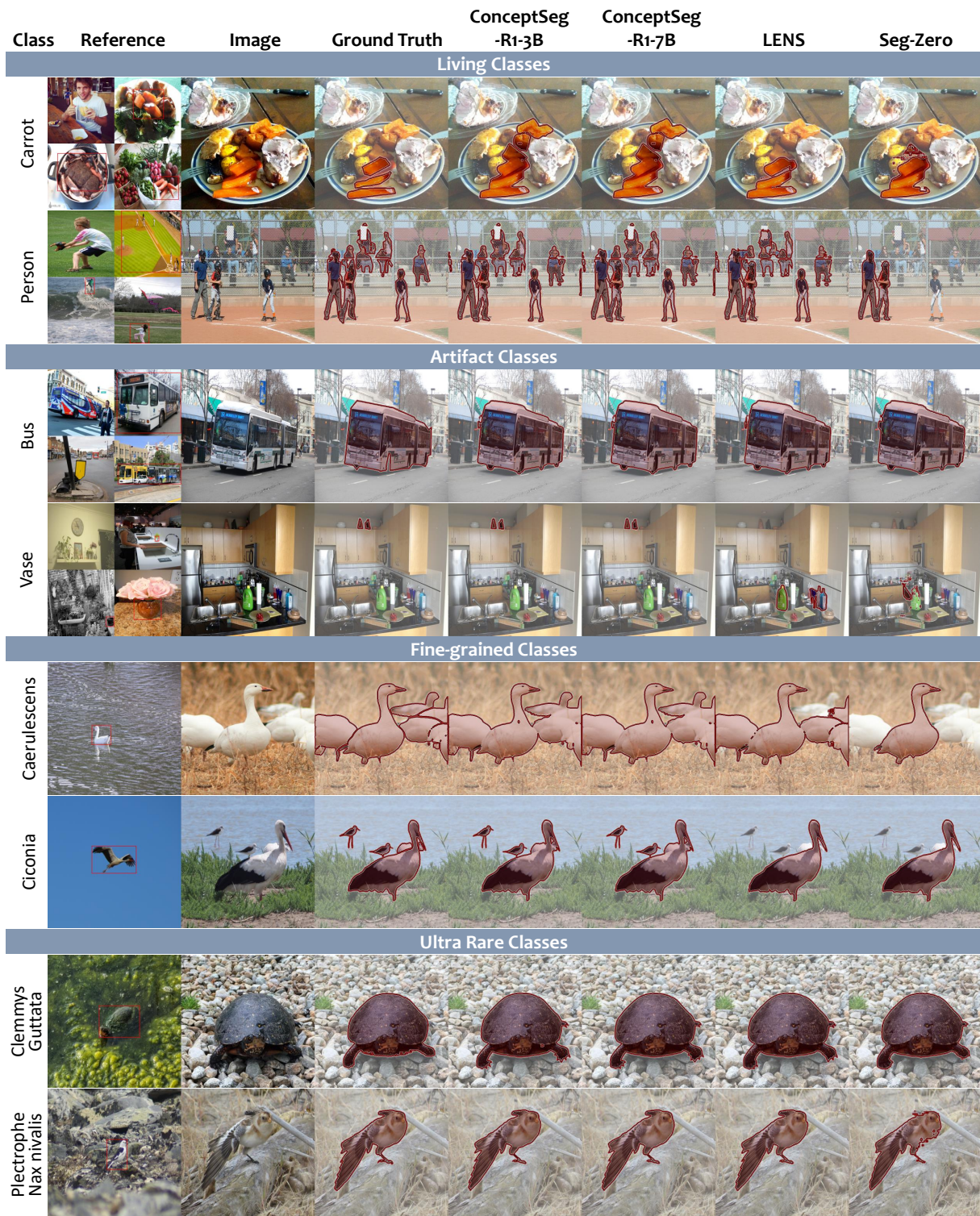
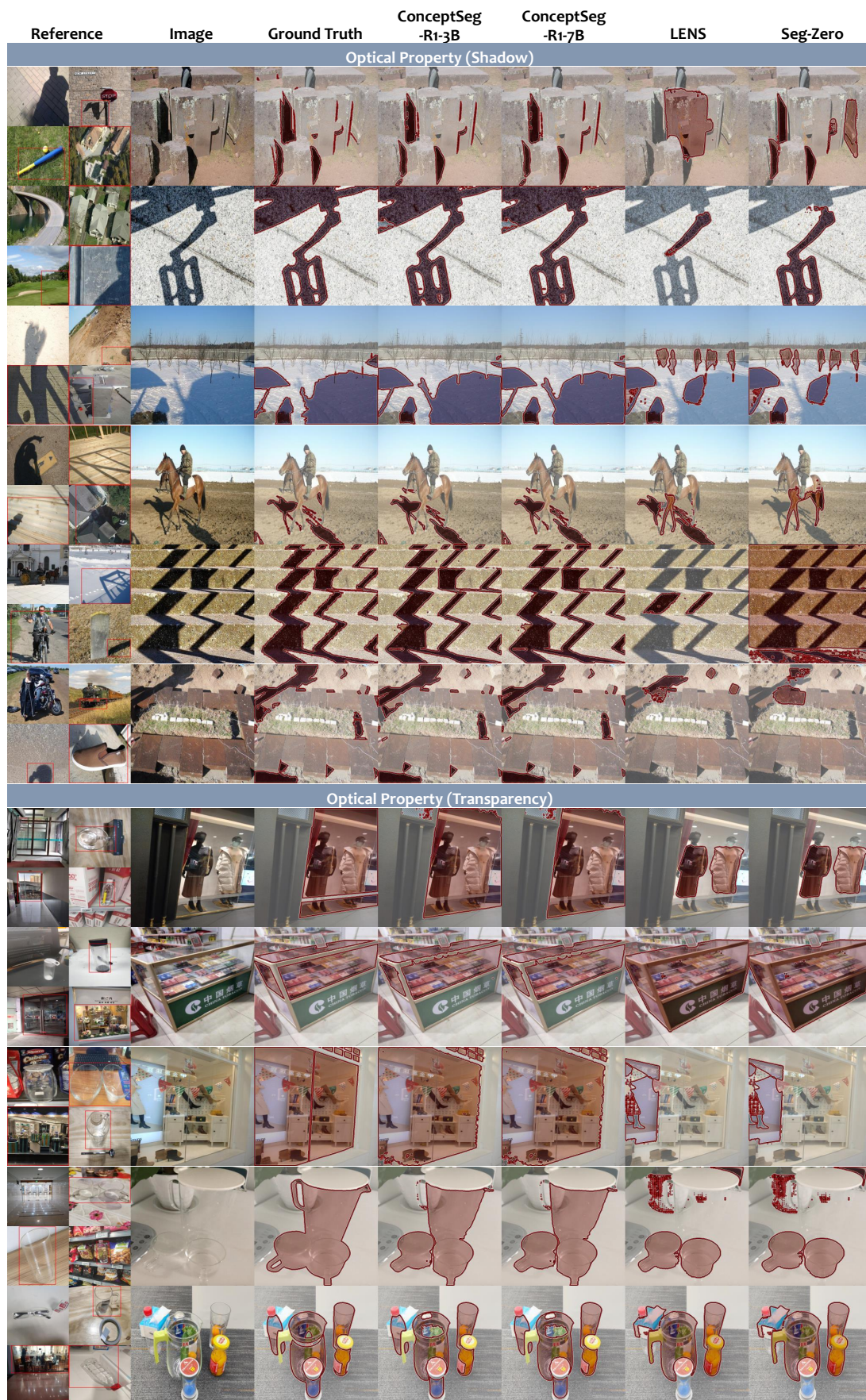


Figure 9. Qualitative comparison on diverse CI concepts.



Referenc Image	Ground Truth	ConceptSeg -R1-3B	ConceptSeg -R1-7B	LENS	Seg-Zero	Think	Rule
Camouflage							
						The task involves identifying objects that are camouflaged in the second image based on the bounding boxes from the first image. In the first image, there are insects and an owl that are segmented. In the second image, there are birds that blend into the environment. The bounding box in the second image should include these birds.	Bounding boxes identify the regions where objects are hidden within their environment.
						The task involves identifying objects that match the segmentation criteria from the reference image in the target image. In the reference image, there are four bounding boxes indicating segmented objects. In the target image, ants are the main objects, but they are not camouflaged. However, the question asks for a camouflaged object, which suggests looking for something less obvious than the ants. Upon closer inspection, there might be some ants that blend into the background due to their size and coloration. The bounding box in the reference image includes a crab, which is not present in the target image. Thus, the ants themselves are the main objects.	Bounding boxes identify objects that are segmented in the first image and then locate similar camouflaged objects in the second image.
						The task involves identifying the camouflaged object in the second image that corresponds to the bounding boxes in the first image. In the first image, there are several animals that blend into their surroundings. In the second image, the seahorse is highly camouflaged against its background. The bounding box in the second image should include the entire seahorse.	Bounding boxes identify the regions where objects are hidden within their environment.
						The task involves identifying the camouflaged object in the second image that corresponds to the bounding boxes in the first image. In the first image, there are three objects that appear to be octopuses or similar creatures. In the second image, there is a single frog that blends into the leaves. The bounding box in the second image should include the frog.	The bounding box in the second image should include the entire frog, ensuring it is segmented correctly.
						The task involves identifying objects that match the segmentation criteria from the reference image in the target image. In the reference image, there are specific bounding boxes indicating objects that need to be segmented. In the target image, the presence of a centipede suggests that the task is to identify its bounding box. The bounding box in the reference image includes parts of the centipede in the target image, which should be segmented.	Bounding boxes in the reference image indicate the presence of specific objects that need to be camouflaged in the target image.
						The task involves identifying the camouflaged object in the second image that corresponds to the bounding boxes in the first image. In the first image, there are three bounding boxes indicating objects that blend into their surroundings. In the second image, the insect appears to be well-camouflaged against the tree trunk. The bounding box in the second image should include the insect.	Bounding boxes identify the regions where the object is located and matches the camouflage in the second image.
Saliency							
						The salient objects in the reference image include animals and a person. In the target image, the child is the most prominent object. The bounding box should include the child and any significant elements like toys or the floor. The bounding box for the child is straightforward, but ensuring the bounding box includes the entire child and some context around them is important.	Bounding boxes are centered on the main objects in the image.
						The salient objects in the reference image include the dog, person, truck, and panda. In the target image, the group of people standing in front of the terraced landscape is the most prominent. The bounding box should include these individuals. The bounding box in the reference image is indicative of the salient objects, so I will use that as a guide.	Bounding boxes identify the main objects in the image.
						The salient objects in the reference image include the woman, the boat, the candle, and the eagle. In the target image, the penguins are the main objects. The bounding boxes in the reference image indicate that we should focus on the main elements in the image. For the target image, the bounding box should include all three penguins.	Bounding boxes identify the main objects in the image.
						The salient objects in the reference image include the cup, egg, woman, and snake. In the target image, the main subjects are the two individuals in the foreground. The bounding boxes should include these individuals and their bicycles. The bounding box for the bicycles needs to be adjusted to include the full extent of the bikes.	Bounding boxes identify the main objects in the image.
						The salient objects in the reference image include the pencil, ladybug, and snail. In the target image, the horses are the most prominent objects. The bounding box should include all the horses. The rule involves identifying the largest and most central objects in the image.	Bounding boxes identify salient objects in the reference image and map them to the target image.
						The salient objects in the reference image include people and an object (a purse). In the target image, the main objects are children playing in a sandbox. The bounding boxes should include the children and their activities. The bounding box in the reference image includes three individuals and one object, which matches the number of bounding boxes in the target image.	Bounding boxes are centered on the main elements in the image.

Figure 11. Qualitative comparison on camouflage and saliency concepts.

Reference Image	Ground Truth	ConceptSeg -R1-3B	ConceptSeg -R1-7B	LENS	Seg-Zero	Think	Rule
Industrial Anomaly							
						The bounding boxes in the reference image indicate specific regions that need to be matched in the target image. The task involves identifying these regions in the target image. The bounding box in the top-left corner of the reference image suggests that the defect is localized in the hand area. In the target image, the entire hand is visible, so the bounding box should include the entire hand. The bounding box in the target image is already covering the entire hand, indicating that the defect is encompassed.	Bounding boxes should cover the entire region of interest in the target image.
						The bounding boxes in the reference image indicate specific regions that contain defects. In the target image, there is a large area with a defect that matches these regions. The bounding box in the reference image includes the areas where the defects are located. Applying the same logic to the target image, I identify the bounding box that corresponds to the defect.	Bounding boxes are used to identify and locate the defective regions in both images.
						The bounding boxes in the reference image indicate specific regions that contain defects. In the target image, there is a single large area that corresponds to these regions. The bounding box in the reference image includes the areas with distinct shapes and textures. Applying the same logic to the target image, I identify the bounding box that matches the defect size and location.	Bounding boxes are identified based on the presence of distinct shapes and textures within the image.
Polyp Lesion							
						The task involves identifying polyps in the colon that correspond to the bounding boxes in the reference image. In the reference image, there are three bounding boxes indicating potential polyps. In the target image, there is a single area that could be interpreted as a polyp due to its irregular shape and size. Applying the bounding box coordinates from the reference image, I identify the target region in the center of the image.	Bounding boxes are used to identify and compare the presence of polyps across images.
						The task involves identifying polyps in the colon that correspond to the bounding boxes in the reference image. In the reference image, there are three bounding boxes indicating potential polyps. In the target image, the presence of a single large structure suggests a single polyp. The bounding box in the reference image is indicative of the location of the polyp, which should be mapped to the target image. The bounding box in the reference image corresponds to the area where the polyp would be located.	Bounding boxes in the reference image map to the location of the polyp in the target image.
						The task involves identifying the presence of polyps in the colon images. In the reference image, there are bounding boxes indicating specific areas where polyps might be located. In the target image, there is a single red spot that could represent a polyp. The bounding box in the reference image suggests that the polyps are relatively small and localized. Applying the bounding box coordinates from the reference image to the target image, I identify the red spot as the equivalent object.	Bounding boxes in the reference image indicate the presence of polyps, which are then matched in the target image based on color and location.
Skin Lesion							
						The task involves identifying the skin lesion in the target image that corresponds to the bounding boxes in the reference image. The bounding boxes in the reference image indicate specific areas of interest on the skin. In the target image, there is a single large lesion that matches the size and location of the bounding boxes in the reference image. Therefore, the bounding box in the target image should be centered on this lesion.	Bounding boxes in the reference image identify the lesion locations, which are then matched in the target image.
						The reference image contains multiple bounding boxes indicating skin lesions. In the target image, there is a single large lesion that matches the size and shape of the bounding boxes in the reference image. The bounding box in the reference image is indicative of the lesion in the target image. The bounding box in the target image should be centered on this lesion.	Bounding boxes in the reference image indicate the presence of lesions. The target image has one large lesion that corresponds to these bounding boxes.
						The task involves identifying the skin lesion in the target image that corresponds to the bounding boxes in the reference image. The bounding boxes in the reference image indicate areas of interest within the skin lesions. In the target image, there is a single lesion that matches the size and shape of the bounding box in the reference image. The bounding box in the target image should be centered on this lesion.	Bounding boxes in the target image should match the size and location of the lesions in the reference image.
Breast Lesion							
						The bounding boxes in the reference image indicate specific regions that correspond to potential breast tumors. In the target image, there is a single large area that matches the size and shape of these bounding boxes. The bounding box in the reference image is indicative of the tumor location, and the target image has a single large structure that fits this description. Thus, the bounding box in the target image should be centered on this large structure.	Bounding boxes in the reference image identify the tumor locations, and the target image should contain a single large structure that corresponds to these.
						The bounding boxes in the reference image indicate specific regions that correspond to potential breast tumors. In the target image, there is a large, irregularly shaped mass that matches the size and location of the bounding boxes in the reference image. The bounding box in the target image should be centered on this mass.	Bounding boxes in the reference image identify the tumor locations, which are then matched in the target image.
						The bounding boxes in the reference image indicate areas that might correspond to breast tumors. In the target image, there is a single area with a marked region that could be indicative of a tumor. The bounding box in the reference image suggests that the tumor is located within a specific area, which in the target image corresponds to the central area with the marked region. The bounding box in the target image should include this marked region.	Bounding boxes in the reference image identify the tumor location, and the target image should include the marked region as the bounding box.

Figure 12. Qualitative comparison on industrial anomaly and medical lesion concepts.

Problem	Reference	Image	Ground Truth	ConceptSeg -R1-3B	ConceptSeg -R1-7B	LENS	Seg-Zero	Think	Rule
Common Consistency									
These images share one object in common. Recognize and locate this object in the last image.								The main object in both images is the bicycle. In the first image, there are multiple bicycles parked or being used by individuals. In the second image, there is a single cyclist riding a bicycle. The task is to identify the shared object, which is the bicycle.	Identify the presence of bicycles in both images.
								The task involves identifying a common object between the two images. In the first image, there are multiple stuffed animals, including a bear and others. In the second image, there is also a stuffed animal, which appears to be a bear. The bounding box should include the entire stuffed animal.	The bounding box should include the entire stuffed animal.
Correspondence Consistency									
For the area marked by the red bounding box in the first image, identify and locate the corresponding area in the second image that serves a similar function or shares a similar meaning.								The bounding box in the first image indicates a side mirror, which is typically used for visibility while driving. In the second image, there is also a side mirror on the car, which serves the same function. The bounding box in the second image should include the side mirror.	The bounding box in the first image includes the side mirror, which needs to be located in the second image.
								The red bounding box in the first image indicates the dog's tongue. In the second image, there is also a dog with its tongue out. Therefore, I need to locate the bounding box for the dog's tongue in the second image.	The bounding box should be centered on the dog's tongue.
Reference Consistency									
Find and locate where does the object in image-1 locate in the image-2.								The object in the first image is a chef's hat, which is worn by the person in the second image. The bounding box in the second image should include the area around the head of the person wearing the hat.	The bounding box should include the area of the hat on the person's head.
								The gloves in the first image are bright green and appear to be work gloves. In the second image, there is another glove hanging on the wall that matches the color and size of the gloves in the first image. The bounding box should include the glove in the second image.	The bounding box should include the glove in the second image.
Static Difference									
Compare these two images carefully and give me the coordinates of their difference.								The main change between the two images is the addition of a squirrel on top of the stop sign in the second image. This suggests that the task involves identifying the presence or absence of the squirrel.	Identify the new object introduced in the second image.
								The main change between the two images is the substitution of orange slices with kiwi slices on the plate. This suggests that the task involves identifying the presence or absence of kiwis in the second image.	The kiwis replace the oranges in the second image.
								The main change between the two images appears to be the addition of an orange figurine on the desk in the second image. This suggests that the presence of the figurine is the distinguishing factor.	Identify the new or changed elements in the scene.
View Difference									
Compare these two images carefully and give me the coordinates of their real difference in the second image. Find it and locate it in the second image.								The main change between the two images involves the presence or absence of a bird. In the first image, there is no bird visible, while in the second image, there is a bird perched on the branch. This suggests that the bird is the key difference.	The bird is the distinguishing element between the two images.
								The main change between the two images is the presence of a person walking in the second image that is not present in the first image. The bounding box for the person in the second image should be identified.	Identify the human figure in the second image.
								The main change between the two images involves the presence of a person in the second image that is not present in the first image. This suggests that the bounding box should include the person.	The bounding box should identify the human figure in the second image.

Figure 13. Qualitative comparison on consistency and difference reasoning concepts.

Problem	Reference Image	Image	Ground Truth	ConceptSeg				Think	Rule
				-R1-3B	-R1-7B	LENS	Seg-Zero		
Logical Rationality									
At their time, what might the people in image-1 need for sailing?								The person in the first image appears to be handling ropes on a ship, suggesting they are engaged in sailing activities. In the second image, there is a globe which could represent navigation tools or educational materials related to sailing. However, the bounding box suggests that the object in question should be identified as something more specific like a compass.	Identify the object in the first image that corresponds to the activity in the second image.
See the object in Image-1? Which object in Image-2 can terminate this state? Find it and locate it in the second image.								The first image shows a person sleeping with musical notes around them, suggesting a state of relaxation or sleep. In the second image, there is no direct indication of sleep or relaxation. However, if we interpret the question as finding an object that could terminate the state of sleep (e.g., an alarm clock), the presence of the clock in the second image suggests it could be used to wake someone up.	The presence of an object that could indicate waking up, such as an alarm clock.
For the people in Image-1, at their time, which object on the table of Image-2 may help them travelling around the world?								The individuals in the first image appear to be sailors, suggesting they might use a globe to navigate. In the second image, there is a globe on the desk, which corresponds to the object that could assist them in traveling around the world.	Identify the globe in the second image as the object that matches the sailors' need for navigation.
Carefully look at the texture of the object in Image-1, which is the real appropriate object to get it into the wood? Find it in Image-2.								The task involves identifying the screw from the first image and locating it in the second image. In the first image, there is a single screw that has been driven into the wood. In the second image, there are various tools and objects, but the screwdriver is the tool typically used to drive screws. The bounding box should include the screwdriver.	Identify the screw in the first image and locate the screwdriver in the second image.
For the people working hard in the hazardous construction site, locate the object on the table of Image-2 to keep him safer.								The individuals in the first image are working on a construction site, which involves potential hazards like falling objects or sharp tools. In the second image, there are various tools laid out on a table. To ensure safety, a helmet should be worn by the workers. The helmet in the second image is located near the bottom left.	Identify the helmet in the second image as the protective gear needed for the workers.
Which object in Image-2 can contribute to the activity the people of Image-1 conducting?								The activity in the first image involves stretching or yoga, which requires a ball for support. In the second image, there is a blue exercise ball that could be used for such activities.	Identify the presence of an exercise ball in the second image.
Which object in Image-2 can effectively solve the messy state of Image-1? Locate it in Image-2.								The task involves identifying an object from Image-2 that could organize the stack of papers in Image-1. In Image-2, there is a stapler which could be used to bind the papers together. The bounding box for the stapler is identified.	The stapler in Image-2 is the object that can organize the papers.
Cross-View Spatio-temporality									
These images share one object in common (the object marked with red bounding box in the first image. Recognize and locate this object in the last image.								The red bounding box in the first image indicates a small table or stool. In the second image, there is a similar object near the center of the room that matches the size and shape of the bounding box in the first image. The bounding box in the second image corresponds to this object.	The bounding box in the first image is used to identify the object, which is then located in the second image by its position and size.
								The red bounding box in the first image indicates a bottle being held by the person, which matches the red bounding box in the second image. The bounding box in the second image corresponds to this bottle.	The bounding box in the first image identifies the object as a bottle of canola oil, and in the second image, it is the same object being held.
								The red bounding box in the first image indicates a microwave oven. In the second image, there is also a microwave oven located above the stove. The bounding box coordinates in the second image should be adjusted to include the microwave.	The bounding box coordinates for the microwave in the second image need to be identified and matched with the red bounding box in the first image.
Cross-Frame Spatio-temporality									
These are a sequence of images containing moving objects. For the object in the first image marked with red bounding box, please locate it in the last image.								The bounding box in the first image indicates an object that seems to be a small animal or dog near the center. In the second image, there is a black dog that matches the location and size of the bounding box in the first image. Thus, I am identifying the dog as the object to locate.	The bounding box coordinates in the first image are used to identify the presence of the dog in the second image.
								The bounding box in the first image indicates a person lying on the ground, which suggests that this individual is the focus of the red bounding box. In the second image, there is no one lying down, but there is a person standing who seems to be the equivalent of the first image's subject. Thus, I am looking for the standing figure.	The bounding box in the first image is adjusted to identify the standing figure in the second image.

Figure 14. Qualitative comparison on logical rationality and spatio-temporality reasoning concepts.

References

- [1] Jonathan Long, Evan Shelhamer, and Trevor Darrell. Fully convolutional networks for semantic segmentation. In *CVPR*, pages 3431–3440, 2015.
- [2] Liang-Chieh Chen, Yukun Zhu, George Papandreou, Florian Schroff, and Hartwig Adam. Encoder-decoder with atrous separable convolution for semantic image segmentation. In *ECCV*, pages 801–818, 2018.
- [3] Enze Xie, Wenhai Wang, Zhiding Yu, Anima Anandkumar, Jose M Alvarez, and Ping Luo. Segformer: Simple and efficient design for semantic segmentation with transformers. In *NeurIPS*, pages 12077–12090, 2021.
- [4] Bowen Cheng, Ishan Misra, Alexander G. Schwing, Alexander Kirillov, and Rohit Girdhar. Masked-attention mask transformer for universal image segmentation. In *CVPR*, pages 1290–1299, 2022.
- [5] Alexander Kirillov, Eric Mintun, Nikhila Ravi, Hanzi Mao, Chloe Rolland, Laura Gustafson, Tete Xiao, Spencer Whitehead, Alexander C Berg, Wan-Yen Lo, et al. Segment anything. In *ICCV*, pages 4015–4026, 2023.
- [6] Nicolas Carion, Laura Gustafson, Yuan-Ting Hu, Shoubhik Debnath, Ronghang Hu, Didac Suris, Chaitanya Ryali, Kalyan Vasudev Alwala, Haitham Khedr, Andrew Huang, et al. Sam 3: Segment anything with concepts. In *ICLR*, 2026.
- [7] Lawrence W Barsalou. Context-independent and context-dependent information in concepts. *Memory & cognition*, 10:82–93, 1982.
- [8] Charlotte Martial, David Stawarczyk, and Arnaud D’Argembeau. Neural correlates of context-independent and context-dependent self-knowledge. *Brain and Cognition*, 125:23–31, 2018.
- [9] Thomas Lachmann and Cees Van Leeuwen. Individual pattern representations are context independent, but their collective representation is context dependent. *The Quarterly Journal of Experimental Psychology Section A*, 58:1265–1294, 2005.
- [10] Xiaoqi Zhao, Youwei Pang, Wei Ji, Baicheng Sheng, Jiaming Zuo, Lihe Zhang, and Huchuan Lu. Spider: a unified framework for context-dependent concept segmentation. In *ICML*, pages 60906–60926, 2024.
- [11] Xiaoqi Zhao, Youwei Pang, Shijie Chang, Yuan Zhao, Lihe Zhang, Chenyang Yu, Hanqi Liu, Jiaming Zuo, Jinsong Ouyang, Weisi Lin, et al. Inspiring the next generation of segment anything models: Comprehensively evaluate sam and sam 2 with diverse prompts towards context-dependent concepts under different scenes. *arXiv preprint arXiv:2412.01240*, 2024.
- [12] Xinlong Wang, Xiaosong Zhang, Yue Cao, Wen Wang, Chunhua Shen, and Tiejun Huang. Seggpt: Towards segmenting everything in context. In *ICCV*, pages 1130–1140, 2023.
- [13] Jingjing Li, Yue Feng, Yuchen Guo, Jincui Huang, Yongri Piao, Qi Bi, Miao Zhang, Xiaoqi Zhao, Qiang Chen, Shihao Zou, et al. Sam3-i: Segment anything with instructions. In *ACL*, 2026.
- [14] Weiming Zhang, Dingwen Xiao, Songyue Guo, Guangyu Xiang, Shiqi Wen, Minwei Zhao, Lei Chen, and Lin Wang. Tarot-sam3: Training-free sam3 for any referring expression segmentation. *arXiv preprint arXiv:2604.07916*, 2026.
- [15] Yuqi Liu, Bohao Peng, Zhisheng Zhong, Zihao Yue, Fanbin Lu, Bei Yu, and Jiaya Jia. Seg-zero: Reasoning-chain guided segmentation via cognitive reinforcement. *arXiv preprint arXiv:2503.06520*, 2025.
- [16] Lianghui Zhu, Bin Ouyang, Yuxuan Zhang, Tianheng Cheng, Rui Hu, Haocheng Shen, Longjin Ran, Xiaoxin Chen, Li Yu, Wenyu Liu, et al. Lens: Learning to segment anything with unified reinforced reasoning. In *AAAI*, pages 13952–13960, 2026.
- [17] Xin Lai, Zhuotao Tian, Yukang Chen, Yanwei Li, Yuhui Yuan, Shu Liu, and Jiaya Jia. Lisa: Reasoning segmentation via large language model. In *CVPR*, pages 9579–9589, 2024.
- [18] Cong Wei, Yujie Zhong, Haoxian Tan, Yingsen Zeng, Yong Liu, Hongfa Wang, and Yujiu Yang. Instructseg: Unifying instructed visual segmentation with multi-modal large language models. In *ICCV*, pages 20193–20203, 2025.
- [19] Muzhi Zhu, Yuzhuo Tian, Hao Chen, Chunluan Zhou, Qingpei Guo, Yang Liu, Ming Yang, and Chunhua Shen. Segagent: Exploring pixel understanding capabilities in mllms by imitating human annotator trajectories. In *CVPR*, pages 3686–3696, 2025.
- [20] Shengyuan Liu, Liuxin Bao, Qi Yang, Wanting Geng, Boyun Zheng, Chenxin Li, Wenting Chen, Houwen Peng, and Yixuan Yuan. Medsam-agent: Empowering interactive medical image segmentation with multi-turn agentic reinforcement learning. *arXiv preprint arXiv:2602.03320*, 2026.
- [21] Zuyao You and Zuxuan Wu. Seg-r1: Segmentation can be surprisingly simple with reinforcement

- learning. [arXiv preprint arXiv:2506.22624](#), 2025.
- [22] Marius Cordts, Mohamed Omran, Sebastian Ramos, Timo Rehfeld, Markus Enzweiler, Rodrigo Benenson, Uwe Franke, Stefan Roth, and Bernt Schiele. The cityscapes dataset for semantic urban scene understanding. In *CVPR*, pages 3213–3223, 2016.
- [23] Woojeong Jin, Jaeho Lee, Heeseong Shin, Seungho Jang, Junhwan Heo, and Seungryoung Kim. Agentrvos: Reasoning over object tracks for zero-shot referring video object segmentation. [arXiv preprint arXiv:2603.23489](#), 2026.
- [24] Shiu-hong Kao, Chak Ho Huang, Huaiqian Liu, Yu-Wing Tai, and Chi-Keung Tang. Cot-seg: Rethinking segmentation with chain-of-thought reasoning and self-correction. [arXiv preprint arXiv:2601.17420](#), 2026.
- [25] Hanoona Rasheed, Muhammad Maaz, Sahal Shaji, Abdelrahman Shaker, Salman Khan, Hisham Cholakkal, Rao Muhammad Anwer, Eric Xing, Ming-Hsuan Yang, and Fahad S. Khan. Glamm: Pixel grounding large multimodal model. In *CVPR*, pages 13009–13018, 2024.
- [26] Chelsea Finn, Pieter Abbeel, and Sergey Levine. Model-agnostic meta-learning for fast adaptation of deep networks. In *ICML*, pages 1126–1135, 2017.
- [27] Alex Nichol, Joshua Achiam, and John Schulman. On first-order meta-learning algorithms. [arXiv preprint arXiv:1803.02999](#), 2018.
- [28] Sewon Min, Mike Lewis, Luke Zettlemoyer, and Hannaneh Hajishirzi. Metaicl: Learning to learn in context. In *NAACL*, pages 2791–2809, 2022.
- [29] Sanchit Sinha, Yuguang Yue, Victor Soto, Mayank Kulkarni, Jianhua Lu, and Aidong Zhang. Maml-en-llm: Model agnostic meta-training of llms for improved in-context learning. In *KDD*, pages 2711–2720, 2024.
- [30] Zhihong Shao, Peiyi Wang, Qihao Zhu, Runxin Xu, Junxiao Song, Xiao Bi, Haowei Zhang, Mingchuan Zhang, YK Li, Yang Wu, et al. Deepseekmath: Pushing the limits of mathematical reasoning in open language models. [arXiv preprint arXiv:2402.03300](#), 2024.
- [31] Dario Amodei, Chris Olah, Jacob Steinhardt, Paul Christiano, John Schulman, and Dan Mané. Concrete problems in ai safety. [arXiv preprint arXiv:1606.06565](#), 2016.
- [32] Shuai Bai, Keqin Chen, Xuejing Liu, Jialin Wang, Wenbin Ge, Sibao Song, Kai Dang, Peng Wang, Shijie Wang, Jun Tang, Humen Zhong, Yuanzhi Zhu, Mingkun Yang, Zhaohai Li, Jianqiang Wan, Pengfei Wang, Wei Ding, Zheren Fu, Yiheng Xu, Jiabo Ye, Xi Zhang, Tianbao Xie, Zesen Cheng, Hang Zhang, Zhibo Yang, Haiyang Xu, and Junyang Lin. Qwen2.5-vl technical report. [arXiv preprint arXiv:2502.13923](#), 2025.
- [33] Yi-Chia Chen, Wei-Hua Li, Cheng Sun, Yu-Chiang Frank Wang, and Chu-Song Chen. Sam4mllm: Enhance multi-modal large language model for referring expression segmentation. In *ECCV*, pages 323–340, 2024.
- [34] Jiaqi Huang, Zunnan Xu, Jun Zhou, Ting Liu, Yicheng Xiao, Mingwen Ou, Bowen Ji, Xiu Li, and Kehong Yuan. Sam-r1: Leveraging sam for reward feedback in multimodal segmentation via reinforcement learning. In *NeurIPS*, 2025.
- [35] Tao Yang, Qing Zhou, Yanliang Li, and Qi Wang. Discriminative perception via anchored description for reasoning segmentation. In *CVPR*, 2026.
- [36] Lijun Wang, Huchuan Lu, Yifan Wang, Mengyang Feng, Dong Wang, Baocai Yin, and Xiang Ruan. Learning to detect salient objects with image-level supervision. In *CVPR*, pages 136–145, 2017.
- [37] Deng-Ping Fan, Ge-Peng Ji, Guolei Sun, Ming-Ming Cheng, Jianbing Shen, and Ling Shao. Camouflaged object detection. In *CVPR*, pages 2777–2787, 2020.
- [38] Xiang Li, Tianhan Wei, Yau Pun Chen, Yu-Wing Tai, and Chi-Keung Tang. Fss-1000: A 1000-class dataset for few-shot segmentation. In *CVPR*, pages 2869–2878, 2020.
- [39] You Li, Heyu Huang, Chi Chen, Kaiyu Huang, Chao Huang, Zonghao Guo, Zhiyuan Liu, Jinan Xu, Yuhua Li, Ruixuan Li, et al. Migician: Revealing the magic of free-form multi-image grounding in multimodal large language models. In *ACL*, pages 9845–9867, 2025.
- [40] Deng-Ping Fan, Tengpeng Li, Zheng Lin, Ge-Peng Ji, Dingwen Zhang, Ming-Ming Cheng, Huazhu Fu, and Jianbing Shen. Re-thinking co-salient object detection. *IEEE TPAMI*, 44(8):4339–4354, 2021.
- [41] Amirreza Shaban, Shray Bansal, Zhen Liu, Irfan Essa, and Byron Boots. One-shot learning for semantic segmentation. In *BMVC*, 2017.
- [42] Enze Xie, Wenjia Wang, Wenhai Wang, Mingyu Ding, Chunhua Shen, and Ping Luo. Segmenting transparent objects in the wild. In *ECCV*, pages 696–711, 2020.
- [43] Tomás F Yago Vicente, Le Hou, Chen-Ping Yu, Minh Hoai, and Dimitris Samaras. Large-scale training of shadow detectors with noisily-annotated shadow examples. In *ECCV*, pages 816–832,

- 2016.
- [44] Wenqi Cui, Kechen Song, Hu Feng, Xiujian Jia, Shaoning Liu, and Yunhui Yan. Autocorrelation-aware aggregation network for salient object detection of strip steel surface defects. *IEEE TIM*, 72:1–12, 2023.
 - [45] Deng-Ping Fan, Ge-Peng Ji, Tao Zhou, Geng Chen, Huazhu Fu, Jianbing Shen, and Ling Shao. Pranet: Parallel reverse attention network for polyp segmentation. In *MICCAI*, pages 263–273, 2020.
 - [46] Walid Al-Dhabyani, Mohammed Gomaa, Hussien Khaled, and Aly Fahmy. Dataset of breast ultrasound images. *Data in brief*, 28:104863, 2020.
 - [47] Noel Codella, Veronica Rotemberg, Philipp Tschandl, M Emre Celebi, Stephen Dusza, David Gutman, Brian Helba, Aadi Kaloo, Konstantinos Liopyris, Michael Marchetti, et al. Skin lesion analysis toward melanoma detection 2018: A challenge hosted by the international skin imaging collaboration (isic). *arXiv preprint arXiv:1902.03368*, 2019.
 - [48] Ilya Loshchilov and Frank Hutter. Decoupled weight decay regularization. In *ICLR*. OpenReview.net, 2019.